UNIVERSIDAD DE CONCEPCIÓN

Centro de Investigación en Ingeniería Matemática (CI^{2}MA)

Nonlinear twofold saddle point-based mixed finite element methods for a regularized $mu(I)$-rheology model of granular materials

Sergio Caucao, Gabriel N. Gatica,
Saulo Medrado, Yuri D. Sobral

PREPRINT 2024-01

SERIE DE PRE-PUBLICACIONES

Nonlinear twofold saddle point-based mixed finite element methods for a regularized $\mu(I)$-rheology model of granular materials*

Dedicated to Professor Dr. Norbert Heuer on the occasion of his 60th birthday

Sergio Caucao† Gabriel N. Gatica‡ Saulo Medrado§ Yuri D. Sobral¶

Abstract

We propose and analyze new mixed finite element methods for a regularized $\mu(I)$-rheology model of granular flows with an equivalent viscosity depending nonlinearly on the pressure and the euclidean norm of the symmetric part of the velocity gradient. To this end, and besides the velocity, the pressure and the aforementioned strain rate, we introduce a modified stress tensor that includes the convective term, and the skew-symmetric vorticity, as auxiliary tensor unknowns, thus yielding a mixed variational formulation within a Banach spaces framework. Then, the pressure is obtained through an iterative postprocess suggested by the incompressibility condition of the fluid, which allows us to express this unknown in terms of the aforementioned stress and the velocity. A fixed-point strategy combined with a solvability result for a class of nonlinear twofold saddle point operator equations in Banach spaces, are employed to show, along with the classical Banach fixed-point theorem, the well-posedness of the continuous and discrete formulations. In particular, PEERS and AFW elements of order $\ell \geqslant 0$ for the stress, the velocity, and the skew-symmetric vorticity, and piecewise polynomials of degree $\leqslant \ell + n$ (resp. $\leqslant \ell + 1$) for the strain rate with PEERS (resp. with AFW), yield stable Galerkin schemes. Optimal a priori error estimates are derived and associated rates of convergence are established. Finally, numerical results confirming the latter and illustrating the good performance of the methods, are reported.

Keywords: granular flows, nonlinear viscosity, twofold saddle point, mixed finite elements, fixed-point theory, a priori error analysis

Mathematics Subject Classifications (2020): 65N30, 65N12, 65N15, 47H10, 47J26, 76D05, 76T25,

1 Introduction

Granular flows are present in our daily lives in different scales: dust on the streets, pills in flasks or in pharmaceutical production lines and sand, that can be found in beaches and as dunes in deserts, for

*This research was partially supported by ANID-Chile through Centro de Modelamiento Matemático (FB210005), and Fondecyt project 11220393; by Centro de Investigación en Ingeniería Matemática (CI^{2}MA), Universidad de Concepción; and by Grupo de Investigación en Análisis Numérico y Cálculo Científico (GIANuC^2), Universidad Católica de la Santísima Concepción.

†GIANuC^2 and Departamento de Matemática y Física Aplicadas, Universidad Católica de la Santísima Concepción, Casilla 297, Concepción, Chile, email: scaucao@ucsc.cl.

‡CI^{2}MA and Departamento de Ingeniería Matemática, Universidad de Concepción, Casilla 160-C, Concepción, Chile, email: ggatica@ci2ma.udec.cl.

§Departamento de Matemática, Universidade de Brasília, Campus Universitário Darcy Ribeiro, 70910-900 Brasília, DF, Brazil, email: saulo.medrado@aluno.unb.br

¶Departamento de Matemática, Universidade de Brasília, Campus Universitário Darcy Ribeiro, 70910-900 Brasília, DF, Brazil, email: ydsobral@unb.br.

example. Understanding the dynamics of granular flows is of utmost importance, especially if lives are at a threat when large scale granular flows occur, such as in landslides and snow avalanches. The first revolutionary work on the mathematical and computational modelling of granular flows was carried out by Cundall & Strack [19]: they proposed a discrete element method (DEM) technique to model the motion of individual granular particles and their contacts with one-another. With this model, several flows of granular materials were studied with outstanding results [2]. However, large scale granular flows posed, and still pose, a major computational problem, as the computational power to simulate enough particles to capture all the relevant features of large scale flows is still unavailable.

The idea of proposing continuum equations, similar to the Navier-Stokes equations for Newtonian fluids, has always attracted researchers in granular materials. One of the first attempts was carried out in [35], but it was only when the very thorough work in [27], which proposed consistent rheological measurements of granular flow properties, that the foundations of an adequate constitutive formulation for granular materials were properly laid. It was proposed in [31] that the dissipative nature of granular flows was due to frictional behaviour, and that the frictional coefficient μ of the flow was governed by the dimensionless *inertial number* I, that compares the shear and collisional time scales in dense granular flows. There was a lot of excitement in the granular materials community with the proposition of this model, as it would be able to handle large scale granular flows, such as avalanches, landslides, sand dunes, etc., that cannot be simulated in their full scale using discrete particles. Since [31] was published, there have been already several works proposing numerical solutions of the $\mu(I)$-rheology equations in different physical setups [33, 36, 15, 21], but there is still some work to be done both on the model itself and on the numerical techniques that are used to solve the underlying governing equations [5].

The major difficulty imposed by the $\mu(I)$-rheology model is the dependence of the dissipative terms on the pressure of the flow. This will be presented in more detail in the following section. However, it is clear that this poses an extra complication to the numerical algorithms that are normally based on pressure-correction projection schemes [28]. In other words, the strong non-linearity of the $\mu(I)$-rheology model prevents us from guaranteeing in advance successful applications of classical numerical methods, such as primal finite elements and related techniques, which are known to be usually more suitable for linear problems, particularly if they are posed within a Hilbertian framework. In this regard, we find it important to stress that the suitability of Banach spaces-based approaches to analyze the continuous and discrete solvabilities of diverse nonlinear problems in continuum mechanics, including several coupled models, and employing mainly mixed formulations, has been confirmed by a significant amount of contributions in recent years. Brinkman-Forchheimer, Darcy-Forchheimer, Navier-Stokes, Boussinesq, coupled flow-transport, and fluidized beds are some of the respective models addressed, and a non-exhaustive list of the corresponding references includes [6, 10, 13, 14, 16, 17, 18, 25]. Needless to say, the most distinctive feature of a mixed formulation is the incorporation of additional unknowns, usually depending on the original ones of the model, for either analytical or physical reasons.

Furthermore, one of the main advantages of employing a Banach framework is the fact that no augmentation is required, a common "trick" of Hilbert spaces-based formulations to force them to become, for instance, elliptic or strongly monotone, and hence the spaces to which the unknowns belong are the natural ones arising simply from the testing of the equations of the model along with the use of the Cauchy-Schwarz and Hölder inequalities. In this way, simpler and closer to the original physical model formulations are derived. In turn, the main benefits of employing a mixed approach include the derivation of momentum-conservative numerical schemes, and the possibility of obtaining direct approximations of further variables of physical interest, either by incorporating them into the formulation, or by employing a postprocessing formula in terms of the remaining unknowns. In the

particular case of our model of interest, to be described below in Section 2, the above might certainly mean to be able to obtain direct calculations of strain rate tensor, shear rate, inertia number, and vorticity, among other variables of interest, thus avoiding numerical differentiation and its consequent loss of accuracy, to approximate them.

According to the previous discussion, the goal of the present work is to introduce and analyze mixed finite element methods for numerically solving the steady-state $\mu(I)$-rheology equations for granular flows. The work is organized as follows. In the rest of this section we collect some notations to be employed throughout the paper. In Section 2 we describe the mathematical model, which includes the setting of a regularized viscosity, and introduce, besides the velocity and the pressure, the further unknowns to be considered. Next, in Section 3 we develop the mixed variational formulation, which is shown to have a twofold saddle point-type structure. The corresponding solvability analysis is carried out in Section 4 by adopting a fixed-point strategy in terms of the velocity and the pressure, and by employing an abstract result on the well-posedness of Banach spaces-based twofold saddle point operator equations, along with the classical Banach theorem. Lipschitz-continuity and motononicity properties of the viscosity function are also required for the analysis. In turn, in Section 5 we define the associated Galerkin scheme, and assume suitable hypotheses on the finite element subspaces in order to prove the corresponding well-posedness by means of a discrete fixed-point approach. A priori error estimates are also obtained here. Then, specific finite element subspaces satisfying the aforementioned assumptions, are derived in Section 6 by applying a useful connection with the discrete stability of the usual Hilbertian mixed formulation for linear elasticity, and optimal rates of convergence are established as well. Finally, numerical experiments illustrating the theoretical findings are reported in Section 7, whereas the fulfillment of the hypotheses on the viscosity is discussed in Appendix A.

Preliminary notations

In what follows, Ω is a bounded domain of R^n, $n \in \{2,3\}$, with Lipschitz-continuous boundary Γ, and corresponding outward normal denoted $\boldsymbol{\nu}$. Then, we adopt the usual notation for Lebesgue spaces $\mathrm{L}^t(\Omega)$ and Sobolev spaces $\mathrm{W}^{l,t}(\Omega)$ and $\mathrm{W}^{l,t}_0(\Omega)$, with $l \geqslant 0$ and $t \in [1,+\infty)$, whose corresponding norms, either for the scalar and vectorial case, are denoted by $\|\cdot\|_{0,t;\Omega}$ and $\|\cdot\|_{l,t;\Omega}$, respectively. In particular, $\mathrm{W}^{0,t}(\Omega) = \mathrm{L}^t(\Omega)$, and when $t = 2$ we write $\mathrm{H}^l(\Omega)$ instead of $\mathrm{W}^{l,2}(\Omega)$, with the corresponding norm and seminorm denoted by $\|\cdot\|_{l,\Omega}$ and $|\cdot|_{l,\Omega}$, respectively. In addition, given any generic scalar functional space M, we let $\mathbf{M}$ and $\mathbb{M}$ be its vectorial and tensorial counterparts, respectively, whereas $\|\cdot\|$ is employed for the norm of any element or operator whenever there is no confusion about the spaces to which they belong. Also, $\mathbb{I}$ stands for the identity tensor in $\mathrm{R}^{n\times n}$, and, besides denoting the absolute value in R, $|\cdot|$ stands for the Euclidean norms in R^n and $\mathrm{R}^{n\times n}$. In turn, for any vector fields $\mathbf{v} = (v_i)_{i\,=\,1,n}$ and $\mathbf{w} = (w_i)_{i\,=\,1,n}$, we set the gradient, divergence, and tensor product operators, respectively, as

$$\nabla\mathbf{v} := \left(\frac{\partial v_i}{\partial x_j}\right)_{i,j\,=\,1,n}, \quad \mathrm{div}(\mathbf{v}) := \sum_{j\,=\,1}^{n} \frac{\partial v_j}{\partial x_j}, \quad \text{and} \quad \mathbf{v}\otimes\mathbf{w} := (v_i w_j)_{i,j\,=\,1,n}\,.$$

On the other hand, for any tensor fields $\boldsymbol{\tau} = (\tau_{ij})_{i,j\,=\,1,n}$ and $\boldsymbol{\zeta} = (\zeta_{ij})_{i,j\,=\,1,n}$, we let $\mathbf{div}(\boldsymbol{\tau})$ be the divergence operator div acting along the rows of $\boldsymbol{\tau}$, and define the transpose, the trace, the tensor inner product operators, and the deviatoric tensor, respectively, as

$$\begin{gathered}\boldsymbol{\tau}^{\mathtt{t}} = (\tau_{ji})_{i,j\,=\,1,n}, \quad \mathrm{tr}(\boldsymbol{\tau}) = \sum_{i\,=\,1}^{n} \boldsymbol{\tau}_{ii}, \quad \boldsymbol{\tau} : \boldsymbol{\zeta} := \sum_{i,j\,=\,1}^{n} \tau_{ij}\zeta_{ij}\,, \\ \text{and} \qquad \boldsymbol{\tau}^{\mathrm{d}} := \boldsymbol{\tau} - \frac{1}{n}\mathrm{tr}(\boldsymbol{\tau})\,\mathbb{I}\,.\end{gathered} \tag{1.1}$$

Furthermore, given $t \in (1, +\infty)$, we introduce the Banach space

$$\mathbb{H}(\mathbf{div}_t;\Omega) := \Big\{ \boldsymbol{\tau} \in \mathbb{L}^2(\Omega) : \quad \mathbf{div}(\boldsymbol{\tau}) \in \mathbf{L}^t(\Omega) \Big\}, \tag{1.2}$$

which is endowed with the natural norm defined by

$$\|\boldsymbol{\tau}\|_{\mathbf{div}_t;\Omega} := \|\boldsymbol{\tau}\|_{0,\Omega} + \|\mathbf{div}(\boldsymbol{\tau})\|_{0,t;\Omega} \qquad \forall\, \boldsymbol{\tau} \in \mathbb{H}(\mathbf{div}_t;\Omega)\,. \tag{1.3}$$

Then, proceeding as in [22, eq. (1.43), Section 1.3.4] (see also [11, Section 4.1] and [16, Section 3.1]), it is easy to show that for each $t \in \begin{cases} (1,+\infty) & \text{if} \quad n = 2 \\ [6/5,+\infty) & \text{if} \quad n = 3 \end{cases}$, there holds

$$\langle \boldsymbol{\tau}\,\boldsymbol{\nu}, \mathbf{v} \rangle = \int_\Omega \Big\{ \boldsymbol{\tau} : \nabla \mathbf{v} + \mathbf{v} \cdot \mathbf{div}(\boldsymbol{\tau}) \Big\} \qquad \forall\, (\boldsymbol{\tau}, \mathbf{v}) \in \mathbb{H}(\mathbf{div}_t;\Omega) \times \mathbf{H}^1(\Omega)\,, \tag{1.4}$$

where $\langle \cdot, \cdot \rangle$ stands for the duality pairing between $\mathbf{H}^{-1/2}(\Gamma)$ and $\mathbf{H}^{1/2}(\Gamma)$.

2 The mathematical model

We are interested in the flows of granular materials based on the $\mu(I)$-rheology approach introduced in [31]. This rheological model arose from the fundamental hypothesis that the corresponding stresses can be described by a visco-plastic constitutive equation in which the internal friction μ of the material, which governs the yield stress, is not constant and depends on a flow parameter called the inertial number I. In order to introduce the corresponding mathematical model, we consider the flow of particles of constant density ρ_p and diameter d in Ω, denote by $\mathbf{u}$ the velocity of the flow, and assume that the latter is incompressible, that is, the volume fraction ϕ of particles is constant throughout the flow, so that the overall density is $\rho = \phi \rho_p$. The governing equations are then given by:

$$\rho \left(\frac{\partial \mathbf{u}}{\partial t} + (\nabla \mathbf{u})\mathbf{u} \right) = \mathbf{div}(\boldsymbol{\sigma}) + \rho\, \mathbf{g} \quad \text{in} \quad \Omega\,, \tag{2.1}$$

and

$$\mathrm{div}(\mathbf{u}) = 0 \quad \text{in} \quad \Omega\,. \tag{2.2}$$

In turn, the stress tensor $\boldsymbol{\sigma}$ is composed of two terms, a deviatoric one associated to dissipation due to the internal friction of the medium, which is inspired by a Coulomb friction-like law, and an isotropic one related to the pressure p on the medium. More precisely, there holds

$$\boldsymbol{\sigma} = \sqrt{2}\,\mu\, p\, \frac{\mathbf{D}}{|\mathbf{D}|} - p\, \mathbb{I} \quad \text{in} \quad \Omega\,, \tag{2.3}$$

where μ is the internal friction coefficient of the granular continuum, $\mathbf{D}$ is the symmetric part of the velocity gradient, namely

$$\mathbf{D} := \frac{1}{2}\Big(\nabla \mathbf{u} + (\nabla \mathbf{u})^{\mathtt{t}} \Big), \tag{2.4}$$

which is also known as the rate of strain tensor, and

$$|\mathbf{D}| = \sqrt{\mathbf{D} : \mathbf{D}}\,. \tag{2.5}$$

Note, thanks to the incompressibility condition (2.2), that there holds

$$\mathrm{tr}(\mathbf{D}) = \mathrm{div}(\mathbf{u}) = 0\,. \tag{2.6}$$

Now, if the friction coefficient is constant, we have the traditional Coulomb model for granular materials [32]. However, there is strong evidence [27] that μ actually depends on the local properties of the flow through the inertial number I, in the form

$$\mu(I) \,:=\, \mu_s + \left(\frac{\mu_d - \mu_s}{I + I_0}\right) I \qquad \text{with} \qquad I = \frac{\sqrt{2}\, d\, |\mathbf{D}|}{\sqrt{p/\rho}}\,, \tag{2.7}$$

where the coefficients μ_s and μ_d correspond, respectively, to the static and dynamic friction limits, and I_0 is a reference (experimental) constant. Then, substituting (2.7) in the constitutive relation (2.3), we arrive at

$$\boldsymbol{\sigma} \,=\, \eta(p, |\mathbf{D}|)\, \mathbf{D} \,-\, p\, \mathbb{I} \quad \text{in} \quad \Omega\,, \tag{2.8}$$

where $\eta : \mathrm{R}^+ \times \mathrm{R}^+ \longrightarrow \mathrm{R}^+$ is defined as

$$\eta(\varrho, \omega) \,:=\, \frac{a_1\, \varrho}{\omega} \,+\, \frac{a_2\, \varrho}{a_3\, \sqrt{\varrho} + a_4\, \omega} \qquad \forall\, (\varrho, \omega) \in \mathrm{R}^+ \times \mathrm{R}^+\,, \tag{2.9}$$

with positive coefficients a_i, $i \in \{1, 2, 3, 4\}$, given by

$$a_1 \,:=\, \sqrt{2}\, \mu_s\,, \quad a_2 \,:=\, 2\, d(\mu_d - \mu_s)\,, \quad a_3 \,:=\, \rho^{-1/2}\, I_0\,, \quad \text{and} \quad a_4 \,:=\, \sqrt{2}\, d\,. \tag{2.10}$$

We stress here that the term $\eta(p, |\mathbf{D}|)$ in (2.8), which can be understood as an equivalent viscosity, is singular when $|\mathbf{D}| = 0$. Indeed, it is expected that some regions of the granular flows are static, as granular materials can exhibit a solid-like behavior [2], just as in a sand pile. In this particular case, the flow of grains only happens near the surface of the dunes, while in the inner core of flow, the material remains static (and resist stresses). In this regard, there are different ways to regularize this problem [21]. For instance, one way is to add a small parameter $0 < \varepsilon \ll 1$ to the denominators in (2.9), thus yielding

$$\eta(\varrho, \omega) \,:=\, \frac{a_1\, \varrho}{\omega + \varepsilon} \,+\, \frac{a_2\, \varrho}{a_3\, \sqrt{\varrho} + a_4\, \omega + \varepsilon} \qquad \forall\, (\varrho, \omega) \in \mathrm{R}^+ \times \mathrm{R}^+\,. \tag{2.11}$$

Finally, regarding boundary conditions, and knowing that recent evidence [29] suggests that there can be some slip between the grains and the boundaries, we proceed accordingly and assume this condition for the steady-state regime that we consider below.

In virtue of the above discussion, the governing equations of the stationary model arising from (2.1), (2.2), and (2.8), are given by

$$\begin{aligned} \rho\, (\nabla \mathbf{u})\mathbf{u} \,&=\, \mathbf{div}\big(\eta(p, |\mathbf{D}|)\, \mathbf{D}\big) \,-\, \nabla p \,+\, \rho\, \mathbf{g} \quad \text{in} \quad \Omega\,, \\ \mathrm{div}(\mathbf{u}) \,&=\, 0 \quad \text{in} \quad \Omega\,, \quad \mathbf{u} \,=\, \mathbf{u}_D \quad \text{on} \quad \Gamma\,, \end{aligned} \tag{2.12}$$

where $\mathbf{u}_D \in \mathbf{H}^{1/2}(\Gamma)$ constitutes a non-necessarily null Dirichlet boundary condition for $\mathbf{u}$. In addition, since our main interest is to develop a fully-mixed finite element method for (2.12), we now introduce a modified stress tensor, still denoted $\boldsymbol{\sigma}$, as the further unknown defined by

$$\boldsymbol{\sigma} \,:=\, \eta(p, |\mathbf{D}|)\, \mathbf{D} \,-\, p\, \mathbb{I} \,-\, \rho\, (\mathbf{u} \otimes \mathbf{u})\,. \tag{2.13}$$

In this way, recalling that the overall density is constant, and noting that the incompressibility condition allows us to show that $\mathbf{div}\big(\mathbf{u} \otimes \mathbf{u}\big) \,=\, (\nabla \mathbf{u})\mathbf{u}$, we deduce that the momentum equation can be rewritten as

$$\mathbf{div}(\boldsymbol{\sigma}) \,+\, \rho\, \mathbf{g} \,=\, 0 \quad \text{in} \quad \Omega\,. \tag{2.14}$$

Moreover, applying deviatoric operator (cf. (1.1)) to (2.13), and using (2.6), which obviously yields $\mathbf{D}^{\mathtt{d}} = \mathbf{D}$, we find that

$$\boldsymbol{\sigma}^{\mathtt{d}} := \eta(p, |\mathbf{D}|)\,\mathbf{D} - \rho\,(\mathbf{u}\otimes\mathbf{u})^{\mathtt{d}} \quad \text{in} \quad \Omega\,. \tag{2.15}$$

In turn, applying now matrix trace to (2.13), we obtain an explicit formula for the pressure p in terms of $\boldsymbol{\sigma}$ and $\mathbf{u}$, namely

$$p = -\frac{1}{n}\,\mathrm{tr}\big(\boldsymbol{\sigma} + \rho\,(\mathbf{u}\otimes\mathbf{u})\big)\,. \tag{2.16}$$

We remark here that (2.13) and the incompressibility condition (2.2) are jointly equivalent to (2.15) - (2.16). On the other hand, in order to perform the usual integration by parts procedure required by a mixed formulation, which reduces to be able to test $\nabla\mathbf{u}$, we now decompose $\mathbf{D}$ as

$$\mathbf{D} = \nabla\mathbf{u} - \boldsymbol{\gamma}\,, \tag{2.17}$$

where $\boldsymbol{\gamma}$ is the auxiliary known given by

$$\boldsymbol{\gamma} := \frac{1}{2}\Big(\nabla\mathbf{u} - (\nabla\mathbf{u})^{\mathtt{t}}\Big)\,. \tag{2.18}$$

Note that the diagonal entries of $\boldsymbol{\gamma}$ are all null, and that the off diagonal ones include the components of the vorticity $\nabla\times\mathbf{u}$. Summarizing, (2.12) can be equivalently reformulated as: Find $\mathbf{D}$, $\boldsymbol{\sigma}$, $\mathbf{u}$, p, and $\boldsymbol{\gamma}$ in suitable spaces, to be defined later on, such that

$$\begin{aligned}
\mathbf{D} - \nabla\mathbf{u} + \boldsymbol{\gamma} &= 0 \qquad \text{in} \quad \Omega\,,\\
\eta(p, |\mathbf{D}|)\,\mathbf{D} - \boldsymbol{\sigma}^{\mathtt{d}} - \rho\,(\mathbf{u}\otimes\mathbf{u})^{\mathtt{d}} &= 0 \qquad \text{in} \quad \Omega\,,\\
\mathbf{div}(\boldsymbol{\sigma}) + \mathbf{f} &= 0 \qquad \text{in} \quad \Omega\,,\\
p = -\frac{1}{n}\,\mathrm{tr}\big(\boldsymbol{\sigma} + \rho\,(\mathbf{u}\otimes\mathbf{u})\big) \quad \text{in} \quad \Omega\,, \quad \mathbf{u} &= \mathbf{u}_D \qquad \text{on} \quad \Gamma\,,
\end{aligned} \tag{2.19}$$

where, for sake of generality as well as for convenience of the numerical experiments to be reported later on, we have replaced $\rho\,\mathbf{g}$ by a source term $\mathbf{f}$, which belongs to a space to be precised in due course. We end this section by remarking that, because of (2.2), the datum $\mathbf{u}_D$ must satisfy the compatibility condition

$$\int_\Gamma \mathbf{u}_D\cdot\boldsymbol{\nu} = 0\,. \tag{2.20}$$

3 The continuous formulation

In this section we derive a variational formulation for the system (2.19). To this end, we first proceed analogously to [7, Section 3] and look originally for $\mathbf{u}$ in $\mathbf{H}^1(\Omega)$. In this way, multiplying the first equation of (2.19) by $\boldsymbol{\tau}\in\mathbb{H}(\mathbf{div}_t;\Omega)$, where $t\in\begin{cases}(1,+\infty) & \text{if} \quad n=2\\ [6/5,+\infty) & \text{if} \quad n=3\end{cases}$, and then applying the integration by parts formula (1.4) along with the Dirichlet boundary condition for $\mathbf{u}$, we obtain

$$\int_\Omega \boldsymbol{\tau}:\mathbf{D} + \int_\Omega \mathbf{u}\cdot\mathbf{div}(\boldsymbol{\tau}) + \int_\Omega \boldsymbol{\tau}:\boldsymbol{\gamma} = \langle\boldsymbol{\tau}\,\boldsymbol{\nu}, \mathbf{u}_D\rangle \qquad \forall\,\boldsymbol{\tau}\in\mathbb{H}(\mathbf{div}_t;\Omega)\,. \tag{3.1}$$

We notice that the first and third terms make sense for $\mathbf{D}$, $\boldsymbol{\gamma}\in\mathbb{L}^2(\Omega)$, which, due to the free trace property of $\mathbf{D}$ (cf. (2.6)) and the skew symmetry of $\boldsymbol{\gamma}$ (cf. (2.18)), leads to look for $\mathbf{D}\in\mathbb{L}^2_{\mathtt{tr}}(\Omega)$ and $\boldsymbol{\gamma}\in\mathbb{L}^2_{\mathtt{sk}}(\Omega)$, where

$$\mathbb{L}_{\mathtt{tr}}(\Omega) := \Big\{\mathbf{E}\in\mathbb{L}^2(\Omega): \quad \mathrm{tr}(\mathbf{E}) = 0\Big\}\,, \tag{3.2}$$

and

$$\mathbb{L}_{\mathtt{sk}}(\Omega) := \Big\{ \boldsymbol{\xi} \in \mathbb{L}^2(\Omega) : \quad \boldsymbol{\xi}^{\mathtt{t}} = -\boldsymbol{\xi} \Big\} . \tag{3.3}$$

In turn, since $\mathbf{div}(\boldsymbol{\tau}) \in \mathbf{L}^t(\Omega)$, we realize by Hölder's inequality that the second term from (3.1) is actually well defined for $\mathbf{u} \in \mathbf{L}^{t'}(\Omega)$, where $t' \in (1, +\infty)$ is the conjugate of t. On the other hand, in order to continue the present derivation, we need to introduce the following hypothesis:

(**H.1**) there exist constants η_1, η_2 such that

$$0 < \eta_1 \leqslant \eta(\varrho, \omega) \leqslant \eta_2 \qquad \forall\, (\varrho, \omega) \in \mathrm{R}^+ \times \mathrm{R}^+ . \tag{3.4}$$

Certainly, the above assumption might imply the need to suitably redefine η in (2.11). Next, testing the second equation of (2.19) against $\mathbf{E} \in \mathbb{L}^2_{\mathtt{tr}}(\Omega)$, and using that $\boldsymbol{\zeta}^{\mathtt{d}} : \mathbf{E} = \boldsymbol{\zeta} : \mathbf{E}$ for all $\boldsymbol{\zeta} \in \mathbb{L}^2(\Omega)$, we formally obtain

$$\int_\Omega \eta(p, |\mathbf{D}|)\, \mathbf{D} : \mathbf{E} - \int_\Omega \boldsymbol{\sigma} : \mathbf{E} - \rho \int_\Omega (\mathbf{u} \otimes \mathbf{u}) : \mathbf{E} = 0 , \tag{3.5}$$

which says, thanks to (3.4), that the first term is well defined, whereas the second one makes sense if $\boldsymbol{\sigma}$ is sought in $\mathbb{L}^2(\Omega)$. Regarding the last term, we first notice, thanks to Cauchy-Schwarz's inequality in $\mathrm{L}^2(\Omega)$ and R^n, that there holds

$$\|\mathbf{w} \otimes \mathbf{v}\|_{0,\Omega} \leqslant n^{1/2} \, \|\mathbf{w}\|_{0,4;\Omega} \, \|\mathbf{v}\|_{0,4;\Omega} \qquad \forall\, \mathbf{w},\, \mathbf{v} \in \mathbb{L}^4(\Omega) . \tag{3.6}$$

It follows that

$$\left| \int_\Omega (\mathbf{u} \otimes \mathbf{u}) : \mathbf{E} \right| \leqslant \|(\mathbf{u} \otimes \mathbf{u})\|_{0,\Omega} \, \|\mathbf{E}\|_{0,\Omega} \leqslant n^{1/2} \, \|\mathbf{u}\|^2_{0,4;\Omega} \, \|\mathbf{E}\|_{0,\Omega} , \tag{3.7}$$

from which we deduce that it suffices to consider $t' = 4$, thus looking for $\mathbf{u}$ in $\mathbf{L}^4(\Omega)$ (equivalently $(\mathbf{u} \otimes \mathbf{u}) \in \mathbb{L}^2(\Omega)$), and then $t = 4/3$, whence the test space of (3.1) becomes $\mathbb{H}(\mathbf{div}_{4/3}; \Omega)$. The above suggests to seek $\boldsymbol{\sigma}$ in this same space, which requires $\mathbf{f}$ to belong to $\mathbf{L}^{4/3}(\Omega)$, so that the third equation of (2.19) is tested as

$$\int_\Omega \mathbf{v} \cdot \mathbf{div}(\boldsymbol{\sigma}) = -\int_\Omega \mathbf{f} \cdot \mathbf{v} \qquad \forall\, \mathbf{v} \in \mathbf{L}^4(\Omega) . \tag{3.8}$$

Now, having identified the spaces to which $\boldsymbol{\sigma}$ and $\mathbf{u}$ belong, we realize from the first equation in the last row of (2.19) that the pressure p must be sought in $\mathrm{L}^2(\Omega)$. Furthermore, the symmetry of $\boldsymbol{\sigma}$ (cf. (2.13)) is weakly imposed by

$$\int_\Omega \boldsymbol{\sigma} : \boldsymbol{\xi} = 0 \qquad \forall\, \boldsymbol{\xi} \in \mathbb{L}^2_{\mathtt{sk}}(\Omega) . \tag{3.9}$$

Finally, we resort to the decomposition

$$\mathbb{H}(\mathbf{div}_{4/3}; \Omega) = \mathbb{H}_0(\mathbf{div}_{4/3}; \Omega) \oplus \mathrm{R}\, \mathbb{I} , \tag{3.10}$$

where

$$\mathbb{H}_0(\mathbf{div}_{4/3}; \Omega) := \Big\{ \boldsymbol{\tau} \in \mathbb{H}(\mathbf{div}_{4/3}; \Omega) : \quad \int_\Omega \mathrm{tr}(\boldsymbol{\tau}) = 0 \Big\} . \tag{3.11}$$

In this way, the unknown $\boldsymbol{\sigma}$ can be decomposed as $\boldsymbol{\sigma} = \boldsymbol{\sigma}_0 + c_0\, \mathbb{I}$, where $\boldsymbol{\sigma}_0 \in \mathbb{H}_0(\mathbf{div}_{4/3}; \Omega)$ and, according to the expression for p in (2.19), there holds

$$c_0 := \frac{1}{n\,|\Omega|} \int_\Omega \mathrm{tr}(\boldsymbol{\sigma}) = -\frac{1}{|\Omega|} \int_\Omega p - \frac{\rho}{n\,|\Omega|} \int_\Omega \mathrm{tr}(\mathbf{u} \otimes \mathbf{u}) , \tag{3.12}$$

which means that, given p, the constant c_0 can be computed once the velocity is known. Thus, it only remains to find $\boldsymbol{\sigma}_0$, which can be placed instead of $\boldsymbol{\sigma}$ in (3.5), (3.8), and (3.9) without altering the validity of these equations. Moreover, it is easy to see that for each $\boldsymbol{\tau} \in \mathrm{R}\mathbb{I}$ both sides of (3.1) vanish, in particular the right one because of the compatibility condition (2.20), and hence testing (3.1) against $\boldsymbol{\tau} \in \mathbb{H}(\mathbf{div}_{4/3};\Omega)$ is equivalent to doing it against $\boldsymbol{\tau} \in \mathbb{H}_0(\mathbf{div}_{4/3};\Omega)$. Consequently, redenoting from now on $\boldsymbol{\sigma}_0$ as simply $\boldsymbol{\sigma} \in \mathbb{H}_0(\mathbf{div}_{4/3};\Omega)$, and suitably gathering (3.1), (3.5), (3.8), and (3.9), we deduce the following mixed variational formulation of (2.19): Given $p \in \mathrm{L}^2(\Omega)$, find $(\mathbf{D},\boldsymbol{\sigma},\mathbf{u},\boldsymbol{\gamma}) \in \mathbb{L}^2_{\mathtt{tr}}(\Omega) \times \mathbb{H}_0(\mathbf{div}_{4/3};\Omega) \times \mathbf{L}^4(\Omega) \times \mathbb{L}^2_{\mathtt{sk}}(\Omega)$ such that

$$
\begin{array}{rcl}
\displaystyle\int_\Omega \eta(p,|\mathbf{D}|)\,\mathbf{D}:\mathbf{E} - \int_\Omega \boldsymbol{\sigma}:\mathbf{E} - \rho\int_\Omega (\mathbf{u}\otimes\mathbf{u}):\mathbf{E} &=& 0\,, \\
\displaystyle -\int_\Omega \boldsymbol{\tau}:\mathbf{D} - \int_\Omega \mathbf{u}\cdot\mathbf{div}(\boldsymbol{\tau}) - \int_\Omega \boldsymbol{\tau}:\boldsymbol{\gamma} &=& -\langle \boldsymbol{\tau}\,\boldsymbol{\nu}, \mathbf{u}_D\rangle\,, \\
\displaystyle -\int_\Omega \mathbf{v}\cdot\mathbf{div}(\boldsymbol{\sigma}) - \int_\Omega \boldsymbol{\sigma}:\boldsymbol{\xi} &=& \displaystyle\int_\Omega \mathbf{f}\cdot\mathbf{v}\,,
\end{array}
\tag{3.13}
$$

for all $(\mathbf{E},\boldsymbol{\tau},\mathbf{v},\boldsymbol{\xi}) \in \mathbf{L}^2_{\mathtt{tr}}(\Omega)\times\mathbb{H}_0(\mathbf{div}_{4/3};\Omega)\times\mathbf{L}^4(\Omega)\times\mathbb{L}^2_{\mathtt{sk}}(\Omega)$. Next, in order to emphasize the particular structure of (3.13), we set the spaces

$$
\mathcal{H}_1 := \mathbb{L}^2_{\mathtt{tr}}(\Omega)\,, \quad \mathcal{H}_2 := \mathbb{H}_0(\mathbf{div}_{4/3};\Omega)\,, \quad \text{and} \quad \mathcal{Q} := \mathbf{L}^4(\Omega)\times\mathbb{L}^2_{\mathtt{sk}}(\Omega)\,, \tag{3.14}
$$

which are endowed with the norms

$$
\|\mathbf{E}\|_{\mathcal{H}_1} := \|\mathbf{E}\|_{0,\Omega}\,, \quad \|\boldsymbol{\tau}\|_{\mathcal{H}_2} := \|\boldsymbol{\tau}\|_{\mathbf{div}_{4/3};\Omega}\,, \quad \text{and} \quad \|(\mathbf{v},\boldsymbol{\xi})\|_{\mathcal{Q}} := \|\mathbf{v}\|_{0,4;\Omega} + \|\boldsymbol{\xi}\|_{0,\Omega}\,,
$$

respectively, and introduce the notations

$$
\vec{\mathbf{u}} := (\mathbf{u},\boldsymbol{\gamma})\,, \quad \vec{\mathbf{v}} := (\mathbf{v},\boldsymbol{\xi}) \in \mathcal{Q}\,.
$$

Then, denoting from now on by $[\,\cdot,\cdot\,]$ the duality pairing between X' and X for any Banach space X, the system (3.13) can be rewritten as: Given $p \in \mathrm{L}^2(\Omega)$, find $(\mathbf{D},\boldsymbol{\sigma},\vec{\mathbf{u}}) \in \mathcal{H}_1\times\mathcal{H}_2\times\mathcal{Q}$ such that

$$
\begin{array}{rcll}
[\mathcal{A}_p(\mathbf{D}),\mathbf{E}] + \mathcal{B}_1(\mathbf{E},\boldsymbol{\sigma}) &=& \mathcal{F}_{\mathbf{u}}(\mathbf{E}) & \forall\,\mathbf{E}\in\mathcal{H}_1\,, \\
\mathcal{B}_1(\mathbf{D},\boldsymbol{\tau}) + \mathcal{B}(\boldsymbol{\tau},\vec{\mathbf{u}}) &=& \mathcal{G}(\boldsymbol{\tau}) & \forall\,\boldsymbol{\tau}\in\mathcal{H}_2\,, \\
\mathcal{B}(\boldsymbol{\sigma},\vec{\mathbf{v}}) &=& \mathcal{F}(\vec{\mathbf{v}}) & \forall\,\vec{\mathbf{v}}\in\mathcal{Q}\,,
\end{array}
\tag{3.15}
$$

where the nonlinear operator $\mathcal{A}_p : \mathcal{H}_1 \to \mathcal{H}_1'$, the bilinear forms $\mathcal{B}_1 : \mathcal{H}_1\times\mathcal{H}_2 \to \mathrm{R}$ and $\mathcal{B} : \mathcal{H}_2\times\mathcal{Q} \to \mathrm{R}$, and the functionals $\mathcal{F}_{\mathbf{z}} : \mathcal{H}_1 \to \mathrm{R}$, for each $\mathbf{z} \in \mathbf{L}^4(\Omega)$, $\mathcal{G} : \mathcal{H}_2 \to \mathrm{R}$, and $\mathcal{F} : \mathcal{Q} \to \mathrm{R}$, are defined by

$$
[\mathcal{A}_p(\mathbf{D}),\mathbf{E}] := \int_\Omega \eta(p,|\mathbf{D}|)\,\mathbf{D}:\mathbf{E} \qquad \forall\,\mathbf{D},\,\mathbf{E}\in\mathcal{H}_1\,, \tag{3.16}
$$

$$
\mathcal{B}_1(\mathbf{E},\boldsymbol{\tau}) := -\int_\Omega \boldsymbol{\tau}:\mathbf{E} \qquad \forall\,(\mathbf{E},\boldsymbol{\tau})\in\mathcal{H}_1\times\mathcal{H}_2\,, \tag{3.17}
$$

$$
\mathcal{B}(\boldsymbol{\tau},\vec{\mathbf{v}}) := -\int_\Omega \mathbf{v}\cdot\mathbf{div}(\boldsymbol{\tau}) - \int_\Omega \boldsymbol{\tau}:\boldsymbol{\xi} \qquad \forall\,(\boldsymbol{\tau},\vec{\mathbf{v}})\in\mathcal{H}_2\times\mathcal{Q}\,, \tag{3.18}
$$

$$
\mathcal{F}_{\mathbf{z}}(\mathbf{E}) := \rho\int_\Omega (\mathbf{z}\otimes\mathbf{z}):\mathbf{E} \qquad \forall\,\mathbf{E}\in\mathcal{H}_1\,, \tag{3.19}
$$

$$
\mathcal{G}(\boldsymbol{\tau}) := -\langle \boldsymbol{\tau}\,\boldsymbol{\nu},\mathbf{u}_D\rangle \qquad \forall\,\boldsymbol{\tau}\in\mathcal{H}_2\,, \tag{3.20}
$$

and

$$\mathcal{F}(\vec{\mathbf{v}}) \,:=\, \int_\Omega \mathbf{f}\cdot\mathbf{v} \qquad \forall\, \vec{\mathbf{v}} \,\in\, \mathcal{Q}\,. \tag{3.21}$$

Note that the upper bound of η (cf. (3.4)) guarantees that $\mathcal{A}_p$ is well-defined in the sense that $\mathcal{A}_p(\mathbf{D}) \in \mathcal{H}_1'$ for all $\mathbf{D} \in \mathcal{H}_1$. In turn, regarding the boundedness properties of the above bilinear forms and linear functionals, we employ the Cauchy-Schwarz and Hölder inequalities, along with (3.7), and the continuity of both the normal trace operator in $\mathbb{H}(\mathbf{div}_{4/3};\Omega)$ and the injection $\mathbf{i}_4 : \mathbf{H}^1(\Omega) \to \mathbf{L}^4(\Omega)$, to deduce the existence of positive constants, denoted and given as

$$\begin{aligned} \|\mathcal{B}_1\| \,:=\, 1\,, \qquad \|\mathcal{B}\| \,:=\, 1\,, \qquad \|\mathcal{F}_{\mathbf{z}}\| \,:=\, \rho\, n^{1/2}\, \|\mathbf{z}\|^2_{0,4;\Omega}\,, \\ \|\mathcal{G}\| \,:=\, \max\big\{1, \|\mathbf{i}_4\|\big\}\, \|\mathbf{u}_D\|_{1/2,\Gamma}\,, \quad \text{and} \quad \|\mathcal{F}\| \,:=\, \|\mathbf{f}\|_{0,4/3;\Omega}\,, \end{aligned} \tag{3.22}$$

such that

$$\begin{aligned} |\mathcal{B}_1(\mathbf{E},\boldsymbol{\tau})| &\leqslant \|\mathcal{B}_1\|\, \|\mathbf{E}\|_{\mathcal{H}_1}\, \|\boldsymbol{\tau}\|_{\mathcal{H}_2} && \forall\, (\mathbf{E},\boldsymbol{\tau}) \in \mathcal{H}_1 \times \mathcal{H}_2\,, \\ |\mathcal{B}(\boldsymbol{\tau},\vec{\mathbf{v}})| &\leqslant \|\mathcal{B}\|\, \|\boldsymbol{\tau}\|_{\mathcal{H}_2}\, \|\vec{\mathbf{v}}\|_{\mathcal{Q}} && \forall\, (\boldsymbol{\tau},\vec{\mathbf{v}}) \in \mathcal{H}_2 \times \mathcal{Q}\,, \\ |\mathcal{F}_{\mathbf{z}}(\mathbf{E})| &\leqslant \|\mathcal{F}_{\mathbf{z}}\|\, \|\mathbf{E}\|_{\mathcal{H}_1} && \forall\, \mathbf{E} \in \mathcal{H}_1\,, \\ |\mathcal{G}(\boldsymbol{\tau})| &\leqslant \|\mathcal{G}\|\, \|\boldsymbol{\tau}\|_{\mathcal{H}_2} && \forall\, \boldsymbol{\tau} \in \mathcal{H}_2\,, \quad \text{and} \\ |\mathcal{F}(\vec{\mathbf{v}})| &\leqslant \|\mathcal{F}\|\, \|\vec{\mathbf{v}}\|_{\mathcal{Q}} && \forall\, \vec{\mathbf{v}} \in \mathcal{Q}\,. \end{aligned} \tag{3.23}$$

We stress here that (3.15) can be seen as a twofold saddle point-type formulation with a nonlinear operator $\mathcal{A}_p$. Furthermore, once this system is solved, and because of its dependence on the given p, we propose to update the pressure unknown according to the expression provided in the last row of (2.19). More precisely, bearing in mind that the stress tensor appearing there is actually $\boldsymbol{\sigma} + c_0\,\mathbb{I}$, with $\boldsymbol{\sigma} \in \mathbb{H}_0(\mathbf{div}_{4/3};\Omega)$ being part of the solution of (3.15), and c_0 given by (3.12), we find that the new pressure, say p_N, becomes

$$p_N \,=\, -\frac{1}{n}\,\mathrm{tr}\big(\boldsymbol{\sigma} + \rho\,(\mathbf{u}\otimes\mathbf{u})\big) \,+\, \frac{1}{|\Omega|}\int_\Omega p \,+\, \frac{\rho}{n\,|\Omega|}\int_\Omega \mathrm{tr}(\mathbf{u}\otimes\mathbf{u})\,.$$

Note from the foregoing equation that p_N, and hence all the subsequent updates of it, keep the same mean value of p, that is $\int_\Omega p_N \,=\, \int_\Omega p$, so that from now on we assume a given positive value, say κ, and define

$$\mathrm{L}^2_\kappa(\Omega) \,:=\, \Big\{ q \in \mathrm{L}^2(\Omega) : \quad \int_\Omega q \,=\, \kappa \Big\}\,.$$

In this way, after solving (3.15) with a given $p \in \mathrm{L}^2_\kappa(\Omega)$, we simply define

$$p_N \,=\, -\frac{1}{n}\,\mathrm{tr}\big(\boldsymbol{\sigma} + \rho\,(\mathbf{u}\otimes\mathbf{u})\big) \,+\, \frac{\kappa}{|\Omega|} \,+\, \frac{\rho}{n\,|\Omega|}\int_\Omega \mathrm{tr}(\mathbf{u}\otimes\mathbf{u})\,. \tag{3.24}$$

We will go back to the above when introducing below in Section 4 a suitable fixed-point approach to analyze the solvability of (3.15).

4 The continuous solvability analysis

In this section we employ a fixed-point approach along with an abstract result on the well-posedness of the aforementioned type of nonlinear operator equations in Banach spaces, to analyze the solvability of the mixed variational formulation (3.15).

4.1 The fixed point strategy

We begin by introducing the operator $\mathbf{T} : \mathbf{L}^4(\Omega) \times \mathrm{L}^2_\kappa(\Omega) \longrightarrow \mathbf{L}^4(\Omega) \times \mathrm{L}^2_\kappa(\Omega)$ defined as

$$\mathbf{T}(\mathbf{z}, r) \,:=\, (\mathbf{u}, p) \qquad \forall\, (\mathbf{z}, r) \,\in\, \mathbf{L}^4(\Omega) \times \mathrm{L}^2_\kappa(\Omega)\,, \tag{4.1}$$

where $(\mathbf{D}, \boldsymbol{\sigma}, \vec{\mathbf{u}}) \,:=\, \big(\mathbf{D}, \boldsymbol{\sigma}, (\mathbf{u}, \boldsymbol{\gamma})\big) \in \mathcal{H}_1 \times \mathcal{H}_2 \times \mathcal{Q}$ is the unique solution (to be confirmed later on) of the problem arising from (3.15) when $\mathcal{A}_p$ and the functional $\mathcal{F}_{\mathbf{u}}$ are replaced by $\mathcal{A}_r$ and $\mathcal{F}_{\mathbf{z}}$, respectively, that is

$$\begin{array}{rcll} [\mathcal{A}_r(\mathbf{D}), \mathbf{E}] \;+ \mathcal{B}_1(\mathbf{E}, \boldsymbol{\sigma}) & = & \mathcal{F}_{\mathbf{z}}(\mathbf{E}) & \forall\, \mathbf{E} \in \mathbb{H}_1\,, \\ \mathcal{B}_1(\mathbf{D}, \boldsymbol{\tau}) \;+ \mathcal{B}(\boldsymbol{\tau}, \vec{\mathbf{u}}) & = & \mathcal{G}(\boldsymbol{\tau}) & \forall\, \boldsymbol{\tau} \in \mathbb{H}_2\,, \\ \mathcal{B}(\boldsymbol{\sigma}, \vec{\mathbf{v}}) & = & \mathcal{F}(\vec{\mathbf{v}}) & \forall\, \vec{\mathbf{v}} \in \mathbb{Q}\,, \end{array} \tag{4.2}$$

and p is computed according to (3.24), that is

$$p \,:=\, -\frac{1}{n}\,\mathrm{tr}\big(\boldsymbol{\sigma} + \rho\,(\mathbf{u} \otimes \mathbf{u})\big) \,+\, \frac{\kappa}{|\Omega|} \,+\, \frac{\rho}{n\,|\Omega|}\int_\Omega \mathrm{tr}(\mathbf{u} \otimes \mathbf{u})\,. \tag{4.3}$$

Then, it is readily seen that solving (3.15) is equivalent to finding a fixed point of $\mathbf{T}$, that is $(\mathbf{u}, p) \in \mathbf{L}^4(\Omega) \times \mathrm{L}^2_\kappa(\Omega)$ such that

$$\mathbf{T}(\mathbf{u}, p) \;=\; (\mathbf{u}, p)\,. \tag{4.4}$$

4.2 Well-definedness of the fixed point operator

In this section we prove that the operator $\mathbf{T}$ (cf. (4.1) - (4.2)) is well-defined, for which we make use of the following abstract result establishing sufficient conditions for the well-posedness of a class of twofold saddle point operator equations.

Theorem 4.1. *Let $\mathbf{X}_1$, $\mathbf{X}_2$, and $\mathbf{Y}$ be reflexive and separable Banach spaces, and let $\mathbf{A} : \mathbf{X}_1 \to \mathbf{X}_1'$ be a nonlinear operator, and $\mathbf{B}_1 : \mathbf{X}_1 \times \mathbf{X}_2 \to \mathrm{R}$ and $\mathbf{B} : \mathbf{X}_2 \times \mathbf{Y} \to \mathrm{R}$ be bounded bilinear forms. In addition, let $\mathbf{V}$ be the null space of the operator induced by $\mathbf{B}$, and assume that*

i) *$\mathbf{A}$ is Lipschitz-continuous, that is there exists a positive constant $L_{\mathbf{A}}$ such that*

$$\|\mathbf{A}(\mathbf{r}) - \mathbf{A}(\mathbf{s})\|_{\mathbf{X}_1'} \;\leqslant\; L_{\mathbf{A}}\,\|\mathbf{r} - \mathbf{s}\|_{\mathbf{X}_1} \qquad \forall\, \mathbf{r},\, \mathbf{s} \in \mathbf{X}_1\,,$$

ii) *the family of operators $\big\{\mathbf{A}(\mathbf{t} + \cdot)\big\}_{\mathbf{t} \in \mathbf{X}_1}$ is uniformly strongly monotone, that is there exists a positive constant $\alpha_{\mathbf{A}}$ such that*

$$[\mathbf{A}(\mathbf{t} + \mathbf{r}) - \mathbf{A}(\mathbf{t} + \mathbf{s}), \mathbf{r} - \mathbf{s}] \;\geqslant\; \alpha_{\mathbf{A}}\,\|\mathbf{r} - \mathbf{s}\|^2_{\mathbf{X}_1} \qquad \forall\, \mathbf{t},\, \mathbf{r},\, \mathbf{s} \in \mathbf{X}_1\,,$$

iii *there exists a positive constant β such that*

$$\sup_{\substack{\tau \in \mathbf{X}_2 \\ \tau \neq 0}} \frac{\mathbf{B}(\tau, v)}{\|\tau\|_{\mathbf{X}_2}} \;\geqslant\; \beta\,\|v\|_{\mathbf{Y}} \qquad \forall\, v \in \mathbf{Y}\,,$$

iv) *and there exists a positive constant β_1 such that*

$$\sup_{\substack{\mathbf{r} \in \mathbf{X}_1 \\ \mathbf{r} \neq 0}} \frac{\mathbf{B}_1(\mathbf{r}, \tau)}{\|\mathbf{r}\|_{\mathbf{X}_1}} \;\geqslant\; \beta_1\,\|\tau\|_{\mathbf{X}_2} \qquad \forall\, \tau \in \mathbf{V}\,.$$

Then, for each $(\mathbf{F}_1, \mathbf{F}_2, \mathbf{G}) \in \mathbf{X}_1' \times \mathbf{X}_2' \times \mathbf{Y}'$ *there exists a unique* $(\mathbf{t}, \sigma, u) \in \mathbf{X}_1 \times \mathbf{X}_2 \times \mathbf{Y}$ *such that*

$$\begin{array}{rcll} [\mathbf{A}(\mathbf{t}), \mathbf{s}] \ + \ \mathbf{B}_1(\mathbf{s}, \sigma) & = & \mathbf{F}_1(\mathbf{s}) & \forall\, \mathbf{s} \in \mathbf{X}_1\,, \\ \mathbf{B}_1(\mathbf{t}, \tau) \ + \ \mathbf{B}(\tau, u) & = & \mathbf{F}_2(\tau) & \forall\, \tau \in \mathbf{X}_2\,, \\ \mathbf{B}(\sigma, v) & = & \mathbf{G}(v) & \forall\, v \in \mathbf{Y}\,. \end{array} \tag{4.5}$$

Moreover, there exists a positive constant C*, depending only on* $L_{\mathbf{A}}$*,* $\alpha_{\mathbf{A}}$*,* β*,* β_1*, and the boundedness constant of* $\mathbf{B}_1$*, say* $\|\mathbf{B}_1\|$*, such that*

$$\|(\mathbf{t}, \boldsymbol{\sigma}, \mathbf{u})\|_{\mathbf{X}_1 \times \mathbf{X}_2 \times \mathbf{Y}} \,\leqslant\, C \left\{ \|\mathbf{F}_1\|_{\mathbf{X}_1'} \,+\, \|\mathbf{F}_2\|_{\mathbf{X}_2'} \,+\, \|\mathbf{G}\|_{\mathbf{Y}'} \,+\, \|\mathbf{A}(0)\|_{\mathbf{X}_1'} \right\}. \tag{4.6}$$

Proof. It is a particular case of [12, Theorem 3.4]. □

As already announced, we plan to apply Theorem 4.1 to conclude the well-posedness of (4.2), for which we proceed next to show that the respective hypotheses are satisfied. In particular, for those involving $\mathcal{A}_r$, we need to incorporate additional assumptions on the function η, namely

(**H.2**) with the same positive constants η_1 and η_2 from (**H.1**), there holds

$$0 \,<\, \eta_1 \,\leqslant\, \eta(\varrho, \omega) + \omega\, \frac{\partial}{\partial \omega} \eta(\varrho, \omega) \,\leqslant\, \eta_2 \qquad \forall\, (\varrho, \omega) \in \mathrm{R}^+ \times \mathrm{R}^+\,, \quad \text{and} \tag{4.7}$$

(**H.3**) there exists a positive constant L_η such that

$$\big|\eta(\varrho, \omega) - \eta(\chi, \omega)\big|\, \omega \,\leqslant\, L_\eta\, |\varrho - \chi| \qquad \forall\, \varrho,\, \chi,\, \omega \in \mathrm{R}^+. \tag{4.8}$$

In the Appendix A we prove that η, as defined by (2.11), satisfies (**H.3**) and that, under a suitable modification of its domain, it accomplishes (**H.1**) and (**H.2**) as well.

Then, we can prove the following lemma establishing continuity and strong-monotonicity properties of the nonlinear operator $\mathcal{A}_r$.

Lemma 4.2. *Let* $L_{\mathcal{A}} := 2\eta_2 - \eta_1$ *and* $\alpha_{\mathcal{A}} := \eta_1$*. Then, there holds*

$$\|\mathcal{A}_r(\mathbf{D}) - \mathcal{A}_r(\mathbf{E})\|_{\mathcal{H}_1'} \,\leqslant\, L_{\mathcal{A}}\, \|\mathbf{D} - \mathbf{E}\|_{\mathcal{H}_1} \qquad \forall\, r \in \mathrm{L}^2(\Omega)\,, \quad \forall\, \mathbf{D},\, \mathbf{E} \in \mathcal{H}_1\,, \tag{4.9}$$

$$[\mathcal{A}_r(\mathbf{D}) - \mathcal{A}_r(\mathbf{E}), \mathbf{D} - \mathbf{E}] \,\geqslant\, \alpha_{\mathcal{A}}\, \|\mathbf{D} - \mathbf{E}\|_{\mathcal{H}_1}^2 \qquad \forall\, r \in \mathrm{L}^2(\Omega)\,, \quad \forall\, \mathbf{D},\, \mathbf{E} \in \mathcal{H}_1\,, \tag{4.10}$$

and

$$\big|[\mathcal{A}_r(\mathbf{D}) - \mathcal{A}_q(\mathbf{D}), \mathbf{E}]\big| \,\leqslant\, L_\eta\, \|r - q\|_{0,\Omega}\, \|\mathbf{E}\|_{\mathcal{H}_1} \qquad \forall\, r,\, q \in \mathrm{L}^2(\Omega)\,, \quad \forall\, \mathbf{D},\, \mathbf{E} \in \mathcal{H}_1\,. \tag{4.11}$$

Proof. For the proofs of (4.9) and (4.10) we refer to [26, Theorem 3.8]. In turn, given r, $q \in \mathrm{L}^2(\Omega)$, and $\mathbf{D}$, $\mathbf{E} \in \mathcal{H}_1$, bearing in mind the definition of $\mathcal{A}_r$ (cf. (3.16)), and using (4.8) with $\varrho = r$, $\chi = q$, and $\omega = |\mathbf{D}|$, we deduce that

$$\begin{aligned} \big|[\mathcal{A}_r(\mathbf{D}) - \mathcal{A}_q(\mathbf{D}), \mathbf{E}]\big| \,&=\, \left| \int_\Omega \Big\{ \eta(r, |\mathbf{D}|) - \eta(q, |\mathbf{D}|) \Big\} \mathbf{D} : \mathbf{E} \right| \\ &\leqslant \int_\Omega \big|\eta(r, |\mathbf{D}|) - \eta(q, |\mathbf{D}|)\big|\, |\mathbf{D}|\, |\mathbf{E}| \,\leqslant\, L_\eta \int_\Omega |r - q|\, |\mathbf{E}|\,, \end{aligned}$$

from which, applying Cauchy-Schwarz's inequality, we obtain (4.11) and end the proof. □

We now observe from (4.9) and (4.10) that, for each $r \in \mathrm{L}^2(\Omega)$, $\mathcal{A}_r$ verifies the hypotheses i) and ii) of Theorem 4.1 with the constants $L_{\mathcal{A}}$ and $\alpha_{\mathcal{A}}$ (cf. Lemma 4.2), respectively. In particular, for ii) we simply notice that there holds

$$\begin{aligned}[\mathcal{A}_r(\mathbf{J}+\mathbf{D})-\mathcal{A}_r(\mathbf{J}+\mathbf{E}),\mathbf{D}-\mathbf{E}] \,&=\, [\mathcal{A}_r(\mathbf{J}+\mathbf{D})-\mathcal{A}_r(\mathbf{J}+\mathbf{E}),(\mathbf{D}+\mathbf{J})-(\mathbf{E}+\mathbf{J})] \\ &\geqslant\, \alpha_{\mathcal{A}}\,\|(\mathbf{D}+\mathbf{J})-(\mathbf{E}+\mathbf{J})\|^2_{\mathcal{H}_1} \,=\, \alpha_{\mathcal{A}}\,\|\mathbf{D}-\mathbf{E}\|^2_{\mathcal{H}_1} \qquad \forall\,\mathbf{J},\,\mathbf{D},\,\mathbf{E}\in\mathcal{H}_1\,.\end{aligned}$$

Next, we recall from [25] the following lemma establishing the continuous inf-sup condition for $\mathcal{B}$.

Lemma 4.3. *There exists a positive constant $\widetilde{\beta}$ such that*

$$\sup_{\substack{\boldsymbol{\tau}\in\mathcal{H}_2\\ \boldsymbol{\tau}\neq 0}}\frac{\mathcal{B}(\boldsymbol{\tau},\vec{\mathbf{v}})}{\|\boldsymbol{\tau}\|_{\mathcal{H}_2}} \,\geqslant\, \widetilde{\beta}\,\|\vec{\mathbf{v}}\|_{\mathcal{Q}} \,=\, \widetilde{\beta}\left\{\|\mathbf{v}\|_{0,4;\Omega}+\|\boldsymbol{\xi}\|_{0,\Omega}\right\} \qquad \forall\,\vec{\mathbf{v}}:=(\mathbf{v},\boldsymbol{\xi})\in\mathcal{Q}\,. \tag{4.12}$$

Proof. See [25, Lemma 3.5] for details. □

Regarding the continuous inf-sup condition for $\mathcal{B}_1$, we first observe from the definition of $\mathcal{B}$ (cf. (3.18)) that the null space of its induced operator is given by

$$\mathcal{V} \,:=\, \left\{\boldsymbol{\tau}\in\mathcal{H}_2:\quad \mathbf{div}(\boldsymbol{\tau})=0 \quad\text{and}\quad \boldsymbol{\tau}=\boldsymbol{\tau}^{\mathtt{t}} \quad\text{in}\quad \Omega\right\}.$$

Then, we recall from [24] the following result.

Lemma 4.4. *There exists a positive constant $\widetilde{\beta}_1$ such that*

$$\sup_{\substack{\mathbf{E}\in\mathcal{H}_1\\ \mathbf{E}\neq 0}}\frac{\mathcal{B}_1(\mathbf{E},\boldsymbol{\tau})}{\|\mathbf{E}\|_{\mathcal{H}_1}} \,\geqslant\, \widetilde{\beta}_1\,\|\boldsymbol{\tau}\|_{\mathcal{H}_2} \qquad \forall\,\boldsymbol{\tau}\in\mathcal{V}\,. \tag{4.13}$$

Proof. See [24, Lemma 3.3] for details. □

We remark here that the proof of Lemma 4.4 makes use of the inequality establishing the existence of a positive constant c_1 such that

$$c_1\,\|\boldsymbol{\tau}\|_{0,\Omega} \,\leqslant\, \|\boldsymbol{\tau}^{\mathtt{d}}\|_{0,\Omega}+\|\mathbf{div}(\boldsymbol{\tau})\|_{0,4/3;\Omega} \qquad \forall\,\boldsymbol{\tau}\in\mathbb{H}_0(\mathbf{div}_{4/3};\Omega)\,. \tag{4.14}$$

The well-posedness of (4.2), equivalently the well-definedness of $\mathbf{T}$, is stated now as follows.

Theorem 4.5. *For each $(\mathbf{z},r)\in\mathbf{L}^4(\Omega)\times\mathrm{L}^2_\kappa(\Omega)$ there exists a unique $(\mathbf{D},\boldsymbol{\sigma},\vec{\mathbf{u}}) := \big(\mathbf{D},\boldsymbol{\sigma},(\mathbf{u},\boldsymbol{\gamma})\big)\in\mathcal{H}_1\times\mathcal{H}_2\times\mathcal{Q}$ solution to (4.2), and hence one can define $\mathbf{T}(\mathbf{z},r) := (\mathbf{u},p)\in\mathbf{L}^4(\Omega)\times\mathrm{L}^2_\kappa(\Omega)$, where p is computed according to (4.3). Moreover, there exists a positive constant $C_{\mathbf{T}}$, depending only on $L_{\mathcal{A}}$, $\alpha_{\mathcal{A}}$, $\widetilde{\beta}$, $\widetilde{\beta}_1$, n, and $\|\mathbf{i}_4\|$, such that*

$$\|\mathbf{u}\|_{0,4;\Omega} \,\leqslant\, \|(\mathbf{D},\boldsymbol{\sigma},\vec{\mathbf{u}})\|_{\mathcal{H}_1\times\mathcal{H}_2\times\mathcal{Q}} \,\leqslant\, C_{\mathbf{T}}\left\{\rho\,\|\mathbf{z}\|^2_{0,4;\Omega}+\|\mathbf{u}_D\|_{1/2,\Gamma}+\|\mathbf{f}\|_{0,4/3;\Omega}\right\}. \tag{4.15}$$

Proof. Having already checked that (4.2) verifies the assumptions i) and ii) of Theorem 4.1, and noting that Lemmas 4.3 and 4.4 confirm that ii) and iv) also hold, the proof is a straightforward application of that abstract result. In particular, the a priori estimate (4.15) follows from (4.6), the boundedness properties of the functionals involved (cf. (3.22), (3.23)), and the fact that $\mathcal{A}_p(\mathbf{0}) = \mathbf{0}\in\mathcal{H}_1'$. Regarding $C_{\mathbf{T}}$, note that we omit its dependence on $\|\mathcal{B}_1\|$ since this latter value equals 1 (cf. (3.22)). □

4.3 Solvability analysis of the fixed point equation

Knowing that $\mathbf{T}$ is well-defined, we now address the solvability of the fixed-point equation (4.4). We begin the analysis deriving sufficient conditions on $\mathbf{T}$ to map a complete metric subspace of $\mathbf{L}^4(\Omega) \times \mathrm{L}^2_\kappa(\Omega)$ into itself. Indeed, given $\delta > 0$, we set

$$\mathrm{W}(\delta) := \Big\{ \mathbf{z} \in \mathbf{L}^4(\Omega) : \quad \|\mathbf{z}\|_{0,4;\Omega} \leqslant \delta \Big\} \quad \text{and} \quad \mathrm{S}(\delta) := \mathrm{W}(\delta) \times \mathrm{L}^2_\kappa(\Omega) \,. \tag{4.16}$$

Then, proceeding as in [7, Lemma 4.7], we are able to prove the following result.

Lemma 4.6. *Assume that*

$$\rho\, \delta \leqslant \frac{1}{2\, C_{\mathbf{T}}} \quad \textit{and} \quad C_{\mathbf{T}} \Big\{ \|\mathbf{u}_D\|_{1/2,\Gamma} + \|\mathbf{f}\|_{0,4/3;\Omega} \Big\} \leqslant \frac{\delta}{2} \,. \tag{4.17}$$

Then, $\mathbf{T}\big(\mathrm{S}(\delta)\big) \subseteq \mathrm{S}(\delta)$.

Proof. Given $(\mathbf{z}, r) \in \mathrm{S}(\delta)$, we know from Theorem 4.5 that $\mathbf{T}(\mathbf{z}, r) := (\mathbf{u}, p)$ is well-defined and that, in virtue of (4.15) and the assumptions from (4.17), there holds

$$\|\mathbf{u}\|_{0,4;\Omega} \leqslant C_{\mathbf{T}} \Big\{ \rho\, \|\mathbf{z}\|^2_{0,4;\Omega} + \|\mathbf{u}_D\|_{1/2,\Gamma} + \|\mathbf{f}\|_{0,4/3;\Omega} \Big\} \leqslant C_{\mathbf{T}}\, \rho\, \delta^2 + \frac{\delta}{2} \leqslant \delta \,,$$

whereas (4.3) guarantees that $p \in \mathrm{L}^2_\kappa(\Omega)$, and hence $(\mathbf{u}, p) \in \mathrm{S}(\delta)$. □

The continuity property of $\mathbf{T}$ is established next.

Lemma 4.7. *Under the same assumption of Lemma* 4.6*, that is* (4.17)*, there exist positive constants* $L_j(\mathbf{T})$*,* $j \in \{1, 2\}$*, depending only on* $L_{\mathcal{A}}$*,* $\alpha_{\mathcal{A}}$*,* $\widetilde{\beta}$*,* $\widetilde{\beta}_1$*,* n*, and* $\|\mathbf{i}_4\|$*, such that*

$$\|\mathbf{T}(\mathbf{z}, r) - \mathbf{T}(\underset{\sim}{\mathbf{z}}, \underset{\sim}{r})\| \leqslant L_1(\mathbf{T})\, \rho\, \delta\, \|\mathbf{z} - \underset{\sim}{\mathbf{z}}\|_{0,4;\Omega} + L_2(\mathbf{T})\, L_\eta\, \|r - \underset{\sim}{r}\|_{0,\Omega} \tag{4.18}$$

for all $(\mathbf{z}, r)$*,* $(\underset{\sim}{\mathbf{z}}, \underset{\sim}{r}) \in \mathrm{S}(\delta)$.

Proof. Given $(\mathbf{z}, r)$, $(\underset{\sim}{\mathbf{z}}, \underset{\sim}{r}) \in \mathrm{S}(\delta)$, we let

$$\mathbf{T}(\mathbf{z}, r) := (\mathbf{u}, p) \quad \text{and} \quad \mathbf{T}(\underset{\sim}{\mathbf{z}}, \underset{\sim}{r}) := (\underset{\sim}{\mathbf{u}}, \underset{\sim}{p}) \,, \tag{4.19}$$

where $(\mathbf{D}, \boldsymbol{\sigma}, \vec{\mathbf{u}}) = \big(\mathbf{D}, \boldsymbol{\sigma}, (\mathbf{u}, \boldsymbol{\gamma})\big) \in \mathcal{H}_1 \times \mathcal{H}_2 \times \mathcal{Q}$ is the unique solution of (4.2) and p is defined by (4.3), and, analogously, $(\underset{\sim}{\mathbf{D}}, \underset{\sim}{\boldsymbol{\sigma}}, \underset{\sim}{\vec{\mathbf{u}}}) = \big(\underset{\sim}{\mathbf{D}}, \underset{\sim}{\boldsymbol{\sigma}}, (\underset{\sim}{\mathbf{u}}, \underset{\sim}{\boldsymbol{\gamma}})\big) \in \mathcal{H}_1 \times \mathcal{H}_2 \times \mathcal{Q}$ is the unique solution of (4.2) with $\mathcal{A}_{\underset{\sim}{r}}$ and $\mathcal{F}_{\underset{\sim}{\mathbf{z}}}$ instead of $\mathcal{A}_r$ and $\mathcal{F}_{\mathbf{z}}$, respectively, and, following (4.3),

$$\underset{\sim}{p} := -\frac{1}{n} \mathrm{tr}\big(\underset{\sim}{\boldsymbol{\sigma}} + \rho\, (\underset{\sim}{\mathbf{u}} \otimes \underset{\sim}{\mathbf{u}})\big) + \frac{\kappa}{|\Omega|} + \frac{\rho}{n\, |\Omega|} \int_\Omega \mathrm{tr}(\underset{\sim}{\mathbf{u}} \otimes \underset{\sim}{\mathbf{u}}) \,. \tag{4.20}$$

Then, subtracting from each other the aforementioned systems (4.2) whose solutions are $(\mathbf{D}, \boldsymbol{\sigma}, \vec{\mathbf{u}})$ and $(\underset{\sim}{\mathbf{D}}, \underset{\sim}{\boldsymbol{\sigma}}, \underset{\sim}{\vec{\mathbf{u}}})$, we obtain

$$\begin{array}{lrcll} [\mathcal{A}_r(\mathbf{D}) - \mathcal{A}_{\underset{\sim}{r}}(\underset{\sim}{\mathbf{D}}), \mathbf{E}] & + \mathcal{B}_1(\mathbf{E}, \boldsymbol{\sigma} - \underset{\sim}{\boldsymbol{\sigma}}) & = & \big(\mathcal{F}_{\mathbf{z}} - \mathcal{F}_{\underset{\sim}{\mathbf{z}}}\big)(\mathbf{E}) & \forall\, \mathbf{E} \in \mathbb{H}_1 \,, \\ \mathcal{B}_1(\mathbf{D} - \underset{\sim}{\mathbf{D}}, \boldsymbol{\tau}) & + \mathcal{B}(\boldsymbol{\tau}, \vec{\mathbf{u}} - \underset{\sim}{\vec{\mathbf{u}}}) & = & 0 & \forall\, \boldsymbol{\tau} \in \mathbb{H}_2 \,, \\ \mathcal{B}(\boldsymbol{\sigma} - \underset{\sim}{\boldsymbol{\sigma}}, \vec{\mathbf{v}}) & & = & 0 & \forall\, \vec{\mathbf{v}} \in \mathbb{Q} \,. \end{array} \tag{4.21}$$

Next, taking $\boldsymbol{\tau} = \boldsymbol{\sigma} - \underset{\sim}{\boldsymbol{\sigma}}$, we get from the second and third rows of the foregoing equation that

$$\mathcal{B}_1(\mathbf{D} - \underset{\sim}{\mathbf{D}}, \boldsymbol{\sigma} - \underset{\sim}{\boldsymbol{\sigma}}) \,=\, -\mathcal{B}(\boldsymbol{\sigma} - \underset{\sim}{\boldsymbol{\sigma}}, \vec{\mathbf{u}} - \vec{\underset{\sim}{\mathbf{u}}}) \,=\, 0\,,$$

which, along with the first row applied to $\mathbf{E} \,=\, \mathbf{D} - \underset{\sim}{\mathbf{D}}$, yields

$$[\mathcal{A}_r(\mathbf{D}) - \mathcal{A}_{\underset{\sim}{r}}(\underset{\sim}{\mathbf{D}}), \mathbf{D} - \underset{\sim}{\mathbf{D}}] \,=\, \big(\mathcal{F}_{\mathbf{z}} - \mathcal{F}_{\underset{\sim}{\mathbf{z}}}\big)(\mathbf{D} - \underset{\sim}{\mathbf{D}})\,.$$

Thus, subtracting and adding $\mathcal{A}_{\underset{\sim}{r}}(\underset{\sim}{\mathbf{D}})$, we see that

$$\begin{aligned}[\mathcal{A}_r(\mathbf{D}) - \mathcal{A}_r(\underset{\sim}{\mathbf{D}}), \mathbf{D} - \underset{\sim}{\mathbf{D}}] &= [\mathcal{A}_r(\mathbf{D}) - \mathcal{A}_{\underset{\sim}{r}}(\underset{\sim}{\mathbf{D}}), \mathbf{D} - \underset{\sim}{\mathbf{D}}] - [\mathcal{A}_r(\underset{\sim}{\mathbf{D}}) - \mathcal{A}_{\underset{\sim}{r}}(\underset{\sim}{\mathbf{D}}), \mathbf{D} - \underset{\sim}{\mathbf{D}}] \\ &= \big(\mathcal{F}_{\mathbf{z}} - \mathcal{F}_{\underset{\sim}{\mathbf{z}}}\big)(\mathbf{D} - \underset{\sim}{\mathbf{D}}) \,-\, [\mathcal{A}_r(\underset{\sim}{\mathbf{D}}) - \mathcal{A}_{\underset{\sim}{r}}(\underset{\sim}{\mathbf{D}}), \mathbf{D} - \underset{\sim}{\mathbf{D}}]\,,\end{aligned}$$

so that, using (4.10) and (4.11), we find that

$$\begin{aligned}\alpha_{\mathcal{A}}\, \|\mathbf{D} - \underset{\sim}{\mathbf{D}}\|_{0,\Omega}^2 \,&\leqslant\, [\mathcal{A}_r(\mathbf{D}) - \mathcal{A}_r(\underset{\sim}{\mathbf{D}}), \mathbf{D} - \underset{\sim}{\mathbf{D}}] \\ &\leqslant\, |\big(\mathcal{F}_{\mathbf{z}} - \mathcal{F}_{\underset{\sim}{\mathbf{z}}}\big)(\mathbf{D} - \underset{\sim}{\mathbf{D}})| \,+\, L_\eta\, \|r - \underset{\sim}{r}\|_{0,\Omega}\, \|\mathbf{D} - \underset{\sim}{\mathbf{D}}\|_{0,\Omega}\,.\end{aligned} \tag{4.22}$$

In turn, it is clear from (3.19) that

$$\big(\mathcal{F}_{\mathbf{z}} - \mathcal{F}_{\underset{\sim}{\mathbf{z}}}\big)(\mathbf{D} - \underset{\sim}{\mathbf{D}}) \,=\, \rho \int_\Omega \big((\mathbf{z} \otimes \mathbf{z}) - (\underset{\sim}{\mathbf{z}} \otimes \underset{\sim}{\mathbf{z}})\big) : (\mathbf{D} - \underset{\sim}{\mathbf{D}})\,, \tag{4.23}$$

from which, subtracting and adding $\underset{\sim}{\mathbf{z}}$ to one of the factors of $(\mathbf{z} \otimes \mathbf{z})$, and using Cauchy-Schwarz's inequality, (3.6), and the fact that $\mathbf{z},\, \underset{\sim}{\mathbf{z}} \in \mathrm{W}(\delta)$, we readily deduce that

$$\begin{aligned}|\big(\mathcal{F}_{\mathbf{z}} - \mathcal{F}_{\underset{\sim}{\mathbf{z}}}\big)(\mathbf{D} - \underset{\sim}{\mathbf{D}})| \,&\leqslant\, n^{1/2}\, \rho\, \big(\|\mathbf{z}\|_{0,4;\Omega} + \|\underset{\sim}{\mathbf{z}}\|_{0,4;\Omega}\big)\, \|\mathbf{z} - \underset{\sim}{\mathbf{z}}\|_{0,4;\Omega}\, \|\mathbf{D} - \underset{\sim}{\mathbf{D}}\|_{0,\Omega} \\ &\leqslant\, 2\, n^{1/2}\, \rho\, \delta\, \|\mathbf{z} - \underset{\sim}{\mathbf{z}}\|_{0,4;\Omega}\, \|\mathbf{D} - \underset{\sim}{\mathbf{D}}\|_{0,\Omega}\,.\end{aligned} \tag{4.24}$$

In this way, employing (4.24) in (4.22), we arrive at

$$\|\mathbf{D} - \underset{\sim}{\mathbf{D}}\|_{0,\Omega} \,\leqslant\, \alpha_{\mathcal{A}}^{-1} \Big\{ 2\, n^{1/2}\, \rho\, \delta\, \|\mathbf{z} - \underset{\sim}{\mathbf{z}}\|_{0,4;\Omega} \,+\, L_\eta\, \|r - \underset{\sim}{r}\|_{0,\Omega} \Big\}\,. \tag{4.25}$$

On the other hand, using the continuous inf-sup condition for $\mathcal{B}$ (cf. (4.12)) and the second row of (4.21), we get

$$\widetilde{\beta}\, \|\vec{\mathbf{u}} - \vec{\underset{\sim}{\mathbf{u}}}\|_{\mathcal{Q}} \,\leqslant\, \sup_{\substack{\boldsymbol{\tau} \in \mathcal{H}_2 \\ \boldsymbol{\tau} \neq 0}} \frac{\mathcal{B}(\boldsymbol{\tau}, \vec{\mathbf{u}} - \vec{\underset{\sim}{\mathbf{u}}})}{\|\boldsymbol{\tau}\|_{\mathcal{H}_2}} \,=\, \sup_{\substack{\boldsymbol{\tau} \in \mathcal{H}_2 \\ \boldsymbol{\tau} \neq 0}} \frac{-\mathcal{B}_1(\mathbf{D} - \underset{\sim}{\mathbf{D}}, \boldsymbol{\tau})}{\|\boldsymbol{\tau}\|_{\mathcal{H}_2}} \,\leqslant\, \|\mathbf{D} - \underset{\sim}{\mathbf{D}}\|_{0,\Omega}\,,$$

which, along with (4.25), implies

$$\|\vec{\mathbf{u}} - \vec{\underset{\sim}{\mathbf{u}}}\|_{\mathcal{Q}} \,\leqslant\, \alpha_{\mathcal{A}}^{-1}\, \widetilde{\beta}^{-1} \Big\{ 2\, n^{1/2}\, \rho\, \delta\, \|\mathbf{z} - \underset{\sim}{\mathbf{z}}\|_{0,4;\Omega} \,+\, L_\eta\, \|r - \underset{\sim}{r}\|_{0,\Omega} \Big\}\,. \tag{4.26}$$

Next, noting from the third row of (4.21) that $\boldsymbol{\sigma} - \underset{\sim}{\boldsymbol{\sigma}}$ belongs to $\mathcal{V} := N(\mathcal{B})$, we have from the continuous inf-sup condition for $\mathcal{B}_1$ (cf. (4.13)) and the first row of (4.21), that

$$\widetilde{\beta}_1\, \|\boldsymbol{\sigma} - \underset{\sim}{\boldsymbol{\sigma}}\|_{\mathcal{H}_2} \,\leqslant\, \sup_{\substack{\mathbf{E} \in \mathcal{H}_1 \\ \mathbf{E} \neq 0}} \frac{\mathcal{B}_1(\mathbf{E}, \boldsymbol{\sigma} - \underset{\sim}{\boldsymbol{\sigma}})}{\|\mathbf{E}\|_{\mathcal{H}_1}} \,=\, \sup_{\substack{\mathbf{E} \in \mathcal{H}_1 \\ \mathbf{E} \neq 0}} \frac{\big(\mathcal{F}_{\mathbf{z}} - \mathcal{F}_{\underset{\sim}{\mathbf{z}}}\big)(\mathbf{E}) - [\mathcal{A}_r(\mathbf{D}) - \mathcal{A}_{\underset{\sim}{r}}(\underset{\sim}{\mathbf{D}}), \mathbf{E}]}{\|\mathbf{E}\|_{\mathcal{H}_1}}\,. \tag{4.27}$$

Then, exactly as for the derivation of (4.24), we deduce that

$$|\big(\mathcal{F}_{\mathbf{z}} - \mathcal{F}_{\underset{\sim}{\mathbf{z}}}\big)(\mathbf{E})| \,\leqslant\, 2\, n^{1/2}\, \rho\, \delta\, \|\mathbf{z} - \underset{\sim}{\mathbf{z}}\|_{0,4;\Omega}\, \|\mathbf{E}\|_{0,\Omega}\,. \tag{4.28}$$

In turn, similarly as previously done in the present proof, it is easily seen that

$$[\mathcal{A}_r(\mathbf{D}) - \mathcal{A}_{\underset{\sim}{r}}(\underset{\sim}{\mathbf{D}}), \mathbf{E}] \,=\, [\mathcal{A}_r(\mathbf{D}) - \mathcal{A}_r(\underset{\sim}{\mathbf{D}}), \mathbf{E}] \,+\, [\mathcal{A}_r(\underset{\sim}{\mathbf{D}}) - \mathcal{A}_{\underset{\sim}{r}}(\underset{\sim}{\mathbf{D}}), \mathbf{E}]\,,$$

from which, employing (4.9) and (4.11), it follows that

$$\big|[\mathcal{A}_r(\mathbf{D}) - \mathcal{A}_{\underset{\sim}{r}}(\underset{\sim}{\mathbf{D}}), \mathbf{E}]\big| \,\leqslant\, \Big\{ L_{\mathcal{A}}\, \|\mathbf{D} - \underset{\sim}{\mathbf{D}}\|_{0,\Omega} \,+\, L_\eta\, \|r - \underset{\sim}{r}\|_{0,\Omega} \Big\}\, \|\mathbf{E}\|_{0,\Omega}\,. \tag{4.29}$$

In this way, replacing the estimates (4.28) and (4.29) back into (4.27), we conclude that

$$\|\boldsymbol{\sigma} - \underset{\sim}{\boldsymbol{\sigma}}\|_{\mathcal{H}_2} \,\leqslant\, \widetilde{\beta}_1^{-1} \Big\{ 2\, n^{1/2}\, \rho\, \delta\, \|\mathbf{z} - \underset{\sim}{\mathbf{z}}\|_{0,4;\Omega} \,+\, L_{\mathcal{A}}\, \|\mathbf{D} - \underset{\sim}{\mathbf{D}}\|_{0,\Omega} \,+\, L_\eta\, \|r - \underset{\sim}{r}\|_{0,\Omega} \Big\}\,, \tag{4.30}$$

which, combined with the estimate for $\|\mathbf{D} - \underset{\sim}{\mathbf{D}}\|_{0,\Omega}$ (cf. (4.25)), leads to

$$\|\boldsymbol{\sigma} - \underset{\sim}{\boldsymbol{\sigma}}\|_{\mathcal{H}_2} \,\leqslant\, \big(1 + L_{\mathcal{A}}\, \alpha_{\mathcal{A}}^{-1}\big)\, \widetilde{\beta}_1^{-1} \Big\{ 2\, n^{1/2}\, \rho\, \delta\, \|\mathbf{z} - \underset{\sim}{\mathbf{z}}\|_{0,4;\Omega} \,+\, L_\eta\, \|r - \underset{\sim}{r}\|_{0,\Omega} \Big\}\,. \tag{4.31}$$

Furthermore, invoking (4.19), (4.3), and (4.20), and performing some simple algebraic computations, which include the use of Cauchy-Schwarz's inequality and the fact that $\|\mathrm{tr}(\boldsymbol{\tau})\|_{0,\Omega} \,\leqslant\, n^{1/2}\, \|\boldsymbol{\tau}\|_{0,\Omega}$, we easily deduce that

$$\|\mathbf{T}(\mathbf{z}, r) - \mathbf{T}(\underset{\sim}{\mathbf{z}}, \underset{\sim}{r})\| \,\leqslant\, \|\mathbf{u} - \underset{\sim}{\mathbf{u}}\|_{0,4;\Omega} \,+\, n^{-1/2}\, \|\boldsymbol{\sigma} - \underset{\sim}{\boldsymbol{\sigma}}\|_{0,\Omega} \,+\, 2\, n^{-1/2}\, \rho\, \|(\mathbf{u} \otimes \mathbf{u}) - (\underset{\sim}{\mathbf{u}} \otimes \underset{\sim}{\mathbf{u}})\|_{0,\Omega}\,, \tag{4.32}$$

from which, subtracting and adding $\mathbf{u}$ to one of the factors of $\mathbf{u} \otimes \mathbf{u}$, employing (3.6), recalling that $\mathbf{u},\ \underset{\sim}{\mathbf{u}} \in \mathrm{W}(\delta)$, and using from (4.17) that $\rho\, \delta \,\leqslant\, \frac{1}{2\, C_{\mathbf{T}}}$, we arrive at

$$\begin{aligned} \|\mathbf{T}(\mathbf{z}, r) - \mathbf{T}(\underset{\sim}{\mathbf{z}}, \underset{\sim}{r})\| \,&\leqslant\, \big(1 \,+\, 4\, \rho\, \delta\big)\, \|\mathbf{u} - \underset{\sim}{\mathbf{u}}\|_{0,4;\Omega} \,+\, n^{-1/2}\, \|\boldsymbol{\sigma} - \underset{\sim}{\boldsymbol{\sigma}}\|_{0,\Omega} \\ &\leqslant\, \big(1 \,+\, 2\, C_{\mathbf{T}}^{-1}\big)\, \|\mathbf{u} - \underset{\sim}{\mathbf{u}}\|_{0,4;\Omega} \,+\, n^{-1/2}\, \|\boldsymbol{\sigma} - \underset{\sim}{\boldsymbol{\sigma}}\|_{0,\Omega}\,. \end{aligned}$$

Finally, replacing the estimates for $\|\mathbf{u} - \underset{\sim}{\mathbf{u}}\|_{0,4;\Omega}$ (cf. (4.26)) and $\|\boldsymbol{\sigma} - \underset{\sim}{\boldsymbol{\sigma}}\|_{0,\Omega}$ (cf. (4.31)) into the foregoing inequality, and recalling from Theorem 4.5 that $C_{\mathbf{T}}$ depends on $L_{\mathcal{A}}$, $\alpha_{\mathcal{A}}$, $\widetilde{\beta}$, $\widetilde{\beta}_1$, n, and $\|\mathbf{i}_4\|$, we conclude the required inequality (4.18) with the constants

$$L_1(\mathbf{T}) \,:=\, 2\, \big(1 + 2\, C_{\mathbf{T}}^{-1}\big)\, \alpha_{\mathcal{A}}^{-1}\, \widetilde{\beta}^{-1}\, n^{1/2} \,+\, 2\, \big(1 + L_{\mathcal{A}}\, \alpha_{\mathcal{A}}^{-1}\big)\, \widetilde{\beta}_1^{-1}$$

and

$$L_2(\mathbf{T}) \,:=\, \big(1 + 2\, C_{\mathbf{T}}^{-1}\big)\, \alpha_{\mathcal{A}}^{-1}\, \widetilde{\beta}^{-1} \,+\, \big(1 + L_{\mathcal{A}}\, \alpha_{\mathcal{A}}^{-1}\big)\, \widetilde{\beta}_1^{-1}\, n^{-1/2}\,.$$

□

We are now in a position to state the first main result of this section.

Theorem 4.8. *Assume that $\rho\, \delta$, L_η, and the data are sufficiently small so that*

$$\begin{gathered} \rho\, \delta \,<\, \min\Big\{ \frac{1}{2\, C_{\mathbf{T}}}, \frac{1}{L_1(\mathbf{T})} \Big\}\,, \qquad L_\eta \,<\, \frac{1}{L_2(\mathbf{T})}\,, \quad \textit{and} \\ C_{\mathbf{T}} \Big\{ \|\mathbf{u}_D\|_{1/2,\Gamma} + \|\mathbf{f}\|_{0,4/3;\Omega} \Big\} \,\leqslant\, \frac{\delta}{2}\,. \end{gathered} \tag{4.33}$$

Then, the operator $\mathbf{T}$ has a unique fixed point $(\mathbf{u}, p) \in \mathrm{S}(\delta)$. Equivalently, given this $p \in \mathrm{L}^2_\kappa(\Omega)$, the system (3.15) *has a unique solution $(\mathbf{D}, \boldsymbol{\sigma}, \vec{\mathbf{u}}) := \big(\mathbf{D}, \boldsymbol{\sigma}, (\mathbf{u}, \boldsymbol{\gamma})\big) \in \mathcal{H}_1 \times \mathcal{H}_2 \times \mathcal{Q}$ with $\mathbf{u} \in \mathrm{W}(\delta)$ and p satisfying* (4.3)*. Moreover, there holds*

$$\|(\mathbf{D}, \boldsymbol{\sigma}, \vec{\mathbf{u}})\|_{\mathcal{H}_1 \times \mathcal{H}_2 \times \mathcal{Q}} \,\leqslant\, 2\, C_{\mathbf{T}} \Big\{ \|\mathbf{u}_D\|_{1/2,\Gamma} \,+\, \|\mathbf{f}\|_{0,4/3;\Omega} \Big\}\,. \tag{4.34}$$

Proof. According to the assumptions stipulated in (4.33), we deduce from Lemmas 4.6 and 4.7 that $\mathbf{T}$ is a contraction mapping $\mathrm{S}(\delta)$ into itself. Hence, a straightforward application of the classical Banach theorem implies the existence of a unique fixed point $(\mathbf{u}, p) \in \mathrm{S}(\delta)$ of this operator, thus yielding the indicated consequences regarding the system (3.15). In turn, thanks to (4.15) (cf. Theorem 4.5) we have

$$\|(\mathbf{D}, \boldsymbol{\sigma}, \vec{\mathbf{u}})\|_{\mathcal{H}_1 \times \mathcal{H}_2 \times \mathcal{Q}} \leqslant C_{\mathbf{T}} \left\{ \rho \, \|\mathbf{u}\|^2_{0,4;\Omega} + \|\mathbf{u}_D\|_{1/2,\Gamma} + \|\mathbf{f}\|_{0,4/3;\Omega} \right\},$$

whereas the fact that $\mathbf{u} \in \mathrm{W}(\delta)$ and the first assumption in (4.33) lead to

$$\rho \, \|\mathbf{u}\|^2_{0,4;\Omega} \leqslant \rho \, \delta \, \|\mathbf{u}\|_{0,4;\Omega} \leqslant \frac{1}{2\, C_{\mathbf{T}}} \, \|(\mathbf{D}, \boldsymbol{\sigma}, \vec{\mathbf{u}})\|_{\mathcal{H}_1 \times \mathcal{H}_2 \times \mathcal{Q}} \,,$$

so that from these two inequalities we readily obtain (4.34) and conclude the proof. □

5 The Galerkin scheme

In this section we introduce the Galerkin scheme of the fully-mixed variational formulation (3.15), analyze its solvability by means of a discrete version of the fixed-point approach employed in Section 4, and derive the corresponding a priori error estimate.

5.1 Preliminaries

We begin by letting $\mathcal{H}_{1,h}$, $\widetilde{\mathcal{H}}_{2,h}$, $\mathcal{Q}_{1,h}$, and $\mathcal{Q}_{2,h}$ be arbitrary finite dimensional subspaces of $\mathbb{L}^2_{\mathtt{tr}}(\Omega)$, $\mathbb{H}(\mathbf{div}_{4/3};\Omega)$, $\mathbf{L}^4(\Omega)$, and $\mathbb{L}^2_{\mathtt{sk}}(\Omega)$, respectively, and let $\mathcal{P}_h := \widetilde{\mathcal{P}}_h \oplus \left\{ \frac{\kappa}{|\Omega|} \right\}$, where $\widetilde{\mathcal{P}}_h$ is a finite dimensional subspace of $\mathrm{L}^2_0(\Omega) := \left\{ q \in \mathrm{L}^2(\Omega) : \quad \int_\Omega q \, = \, 0 \right\}$. Hereafter, h stands for both the sub-index of each subspace and the size of each member of a regular family $\left\{ \mathcal{T}_h \right\}_{h>0}$ of triangulations of $\bar{\Omega}$ made up of triangles K (when $n = 2$) or tetrahedra K (when $n = 3$) of diameters h_K, so that $h := \max \left\{ h_K : \quad K \in \mathcal{T}_h \right\}$. Now, defining

$$\mathcal{H}_{2,h} := \mathbb{H}_0(\mathbf{div}_{4/3};\Omega) \cap \widetilde{\mathcal{H}}_{2,h} \quad \text{ and } \quad \mathcal{Q}_h := \mathcal{Q}_{1,h} \times \mathcal{Q}_{2,h} \,,$$

and letting $p_h \in \mathcal{P}_h$ be a given discrete approximation of the pressure p, the Galerkin scheme associated with (3.15) reads: Find $(\mathbf{D}_h, \boldsymbol{\sigma}_h, \vec{\mathbf{u}}_h) := \big(\mathbf{D}_h, \boldsymbol{\sigma}_h, (\mathbf{u}_h, \boldsymbol{\gamma}_h)\big) \in \mathcal{H}_{1,h} \times \mathcal{H}_{2,h} \times \mathcal{Q}_h$ such that

$$\begin{array}{lrcll} [\mathcal{A}_{p_h}(\mathbf{D}_h), \mathbf{E}_h] & + \mathcal{B}_1(\mathbf{E}_h, \boldsymbol{\sigma}_h) & = & \mathcal{F}_{\mathbf{u}_h}(\mathbf{E}_h) & \forall \, \mathbf{E}_h \in \mathcal{H}_{1,h} \,, \\ \mathcal{B}_1(\mathbf{D}_h, \boldsymbol{\tau}_h) & + \mathcal{B}(\boldsymbol{\tau}_h, \vec{\mathbf{u}}_h) & = & \mathcal{G}(\boldsymbol{\tau}_h) & \forall \, \boldsymbol{\tau}_h \in \mathcal{H}_{2,h} \,, \\ \mathcal{B}(\boldsymbol{\sigma}_h, \vec{\mathbf{v}}_h) & & = & \mathcal{F}(\vec{\mathbf{v}}_h) & \forall \, \vec{\mathbf{v}}_h \in \mathcal{Q}_h \,. \end{array} \tag{5.1}$$

Next, we consider the discrete analogue of the fixed-point strategy employed in Section 4. Indeed, we introduce the discrete operator $\mathbf{T}_h : \mathcal{Q}_{1,h} \times \mathcal{P}_h \to \mathcal{Q}_{1,h} \times \mathcal{P}_h$ defined by

$$\mathbf{T}_h(\mathbf{z}_h, r_h) := (\mathbf{u}_h, p_h) \qquad \forall \, (\mathbf{z}_h, r_h) \, \in \, \mathcal{Q}_{1,h} \times \mathcal{P}_h \,, \tag{5.2}$$

where $(\mathbf{D}_h, \boldsymbol{\sigma}_h, \vec{\mathbf{u}}_h) := \big(\mathbf{D}_h, \boldsymbol{\sigma}_h, (\mathbf{u}_h, \boldsymbol{\gamma}_h)\big) \in \mathcal{H}_{1,h} \times \mathcal{H}_{2,h} \times \mathcal{Q}_h$ is the unique solution (to be confirmed later on) of the problem arising from (5.1) when $\mathcal{A}_{p_h}$ and the functional $\mathcal{F}_{\mathbf{u}_h}$ are replaced by $\mathcal{A}_{r_h}$ and

$\mathcal{F}_{\mathbf{z}_h}$, respectively, that is

$$\begin{array}{lllll} [\mathcal{A}_{r_h}(\mathbf{D}_h),\mathbf{E}_h] & +\mathcal{B}_1(\mathbf{E}_h,\boldsymbol{\sigma}_h) & = & \mathcal{F}_{\mathbf{z}_h}(\mathbf{E}_h) & \forall\, \mathbf{E}_h \in \mathcal{H}_{1,h}\,, \\ \mathcal{B}_1(\mathbf{D}_h,\boldsymbol{\tau}_h) & +\mathcal{B}(\boldsymbol{\tau}_h,\vec{\mathbf{u}}_h) & = & \mathcal{G}(\boldsymbol{\tau}_h) & \forall\, \boldsymbol{\tau}_h \in \mathcal{H}_{2,h}\,, \\ \mathcal{B}(\boldsymbol{\sigma}_h,\vec{\mathbf{v}}_h) & & = & \mathcal{F}(\vec{\mathbf{v}}_h) & \forall\, \vec{\mathbf{v}}_h \in \mathcal{Q}_h\,, \end{array} \tag{5.3}$$

whereas p_h is computed as suggested by the discrete version of (3.24), that is

$$p_h \,:=\, -\frac{1}{n}\,\mathrm{tr}\big(\boldsymbol{\sigma}_h + \rho\,(\mathbf{u}_h\otimes\mathbf{u}_h)\big) \,+\, \frac{\kappa}{|\Omega|} \,+\, \frac{\rho}{n\,|\Omega|}\int_\Omega \mathrm{tr}(\mathbf{u}_h\otimes\mathbf{u}_h)\,. \tag{5.4}$$

Note from (5.4) that the specific subspaces to which $\boldsymbol{\sigma}_h$ and $\mathbf{u}_h$ belong determine the choice of $\widetilde{\mathcal{P}}_h$. Then, it is readily seen that solving (5.1) is equivalent to finding a fixed point of $\mathbf{T}_h$, that is $(\mathbf{u}_h,p_h)\in\mathcal{Q}_{1,h}\times\mathcal{P}_h$ such that

$$\mathbf{T}_h(\mathbf{u}_h,p_h) \,=\, (\mathbf{u}_h,p_h)\,. \tag{5.5}$$

5.2 Discrete solvability analysis

In what follows we proceed analogously to Sections 4.2 and 4.3, and establish the well-posedness of the Galerkin scheme (5.1) by means of the solvability study of the equivalent fixed-point equation (5.5). In this regard, we announce in advance that, being the respective discussion similar to the one developed for the continuous formulation, here we simply collect the main results and provide selected details of their proofs. To this end, suitable hypotheses regarding the arbitrary subspaces $\mathcal{H}_{1,h}$, $\widetilde{\mathcal{H}}_{2,h}$, and $\mathcal{Q}_h$, need to be introduced throughout the analysis. Explicit finite element subspaces satisfying them will be specified later on in Section 6.

We begin by letting $\mathcal{V}_h$ be the discrete kernel of the bilinear form $\mathcal{B}$, that is

$$\mathcal{V}_h \,:=\, \Big\{\boldsymbol{\tau}_h\in\mathcal{H}_{2,h}:\quad \mathcal{B}(\boldsymbol{\tau}_h,\vec{\mathbf{v}}_h) \,=\, 0 \quad \forall\,\vec{\mathbf{v}}_h\in\mathcal{Q}_h\Big\}\,, \tag{5.6}$$

and by assuming that

(**H.4**) $\widetilde{\mathcal{H}}_{2,h}$ contains multiples of the identity tensor $\mathbb{I}$,

(**H.5**) $\mathbf{div}(\widetilde{\mathcal{H}}_{2,h}) \,\subseteq\, \mathcal{Q}_{1,h}$,

(**H.6**) $\mathcal{V}_h^{\mathtt{d}} \,:=\, \Big\{\boldsymbol{\tau}_h^{\mathtt{d}}:\quad \boldsymbol{\tau}_h\in\mathcal{V}_h\Big\} \,\subseteq\, \mathcal{H}_{1,h}$, and

(**H.7**) there exists a positive constant $\widetilde{\beta}_{\mathtt{d}}$, independent of h, such that

$$\sup_{\substack{\boldsymbol{\tau}_h\in\mathcal{H}_{2,h}\\ \boldsymbol{\tau}_h\neq 0}} \frac{\mathcal{B}(\boldsymbol{\tau}_h,\vec{\mathbf{v}}_h)}{\|\boldsymbol{\tau}_h\|_{\mathcal{H}_2}} \,\geqslant\, \widetilde{\beta}_{\mathtt{d}}\,\|\vec{\mathbf{v}}_h\|_{\mathcal{Q}} \,=\, \widetilde{\beta}_{\mathtt{d}}\,\Big\{\|\mathbf{v}_h\|_{0,4;\Omega}+\|\boldsymbol{\xi}_h\|_{0,\Omega}\Big\} \qquad \forall\,\vec{\mathbf{v}}_h:=(\mathbf{v}_h,\boldsymbol{\xi}_h)\in\mathcal{Q}_h\,. \tag{5.7}$$

Then, as a consequence of (**H.4**), there holds the discrete version of the decomposition (3.10), namely $\widetilde{\mathcal{H}}_{2,h} \,=\, \mathcal{H}_{2,h}\oplus\mathrm{R}\mathbb{I}$, which confirms the validity of using $\mathcal{H}_{2,h}$ as the subspace where σ_h is sought. Now, according to the definition of $\mathcal{B}$ (cf. (3.18)), and noting that (**H.5**) can be equivalently rephrased as $\mathbf{div}(\mathcal{H}_{2,h})\subseteq\mathcal{Q}_{1,h}$, it readily follows from (5.6) that

$$\mathcal{V}_h \,:=\, \Big\{\boldsymbol{\tau}_h\in\mathcal{H}_{2,h}:\quad \mathbf{div}(\boldsymbol{\tau}_h)=0 \quad\text{and}\quad \int_\Omega \boldsymbol{\tau}_h:\boldsymbol{\xi}_h \,=\, 0 \quad \forall\,\boldsymbol{\xi}_h\in\mathcal{Q}_{2,h}\Big\}\,, \tag{5.8}$$

which yields the discrete analogue of (4.13). Indeed, given $\boldsymbol{\tau}_h \in \mathcal{V}_h$ such that $\boldsymbol{\tau}_h^{\mathtt{d}} \neq \mathbf{0}$, we have thanks to (**H.6**) that $-\boldsymbol{\tau}_h^{\mathtt{d}} \in \mathcal{H}_{1,h}$, and thus

$$\sup_{\substack{\mathbf{E}_h \in \mathcal{H}_{1,h} \\ \mathbf{E}_h \neq 0}} \frac{\mathcal{B}_1(\mathbf{E}_h, \boldsymbol{\tau}_h)}{\|\mathbf{E}_h\|_{\mathcal{H}_1}} \geqslant \frac{\mathcal{B}_1(-\boldsymbol{\tau}_h^{\mathtt{d}}, \boldsymbol{\tau}_h)}{\|\boldsymbol{\tau}_h^{\mathtt{d}}\|_{\mathcal{H}_1}} = \|\boldsymbol{\tau}_h^{\mathtt{d}}\|_{0,\Omega} ,$$

from which, employing the inequality (4.14), we arrive at

$$\sup_{\substack{\mathbf{E}_h \in \mathcal{H}_{1,h} \\ \mathbf{E}_h \neq 0}} \frac{\mathcal{B}_1(\mathbf{E}_h, \boldsymbol{\tau}_h)}{\|\mathbf{E}_h\|_{\mathcal{H}_1}} \geqslant \widetilde{\beta}_{1,\mathtt{d}} \|\boldsymbol{\tau}_h\|_{\mathcal{H}_1} , \tag{5.9}$$

with $\widetilde{\beta}_{1,\mathtt{d}} = c_1$. Now, if $\boldsymbol{\tau}_h \in \mathcal{V}_h$ is such that $\boldsymbol{\tau}_h^{\mathtt{d}} = \mathbf{0}$, then it follows from (4.14) that $\boldsymbol{\tau}_h = \mathbf{0}$, whence (5.9) holds trivially in this case.

Furthermore, it is not difficult to see that the Lipschitz-continuity and monotoniticity properties of $\mathcal{A}_r$ provided in Lemma 4.2 (cf. (4.9), (4.10), and (4.11)), are also valid in the present discrete case, and with the same constants $L_{\mathcal{A}}$, $\alpha_{\mathcal{A}}$, and L_η, that is

$$\|\mathcal{A}_{r_h}(\mathbf{D}_h) - \mathcal{A}_{r_h}(\mathbf{E}_h)\|_{\mathcal{H}'_{1,h}} \leqslant L_{\mathcal{A}} \|\mathbf{D}_h - \mathbf{E}_h\|_{\mathcal{H}_1} \qquad \forall\, r_h \in \mathcal{P}_h , \quad \forall\, \mathbf{D}_h, \mathbf{E}_h \in \mathcal{H}_{1,h} , \tag{5.10}$$

$$[\mathcal{A}_{r_h}(\mathbf{D}_h) - \mathcal{A}_{r_h}(\mathbf{E}_h), \mathbf{D}_h - \mathbf{E}_h] \geqslant \alpha_{\mathcal{A}} \|\mathbf{D}_h - \mathbf{E}_h\|^2_{\mathcal{H}_1} \qquad \forall\, r_h \in \mathcal{P}_h , \quad \forall\, \mathbf{D}_h, \mathbf{E}_h \in \mathcal{H}_{1,h} , \tag{5.11}$$

and

$$\big|[\mathcal{A}_{r_h}(\mathbf{D}_h) - \mathcal{A}_{q_h}(\mathbf{D}_h), \mathbf{E}_h]\big| \leqslant L_\eta \|r_h - q_h\|_{0,\Omega} \|\mathbf{E}_h\|_{\mathcal{H}_1} \qquad \forall\, r_h, q_h \in \mathcal{P}_h , \quad \forall\, \mathbf{D}_h, \mathbf{E}_h \in \mathcal{H}_{1,h} . \tag{5.12}$$

Consequently, we are now in a position to establish the discrete analogue of Theorem 4.5.

Theorem 5.1. *For each $(\mathbf{z}_h, r_h) \in \mathcal{Q}_{1,h} \times \mathcal{P}_h$ there exists a unique $(\mathbf{D}_h, \boldsymbol{\sigma}_h, \vec{\mathbf{u}}_h) := \big(\mathbf{D}_h, \boldsymbol{\sigma}_h, (\mathbf{u}_h, \boldsymbol{\gamma}_h)\big)$ $\in \mathcal{H}_{1,h} \times \mathcal{H}_{2,h} \times \mathcal{Q}_h$ solution to (5.3), and hence one can define $\mathbf{T}(\mathbf{z}_h, r_h) := (\mathbf{u}_h, p_h) \in \mathcal{Q}_{1,h} \times \mathcal{P}_h$, where p_h is computed according to (5.4). Moreover, there exists a positive constant $C_{\mathbf{T},\mathtt{d}}$, depending only on $L_{\mathcal{A}}$, $\alpha_{\mathcal{A}}$, $\widetilde{\beta}_{\mathtt{d}}$, $\widetilde{\beta}_{1,\mathtt{d}}$, n, and $\|\mathbf{i}_4\|$, such that*

$$\|\mathbf{u}_h\|_{0,4;\Omega} \leqslant \|(\mathbf{D}_h, \boldsymbol{\sigma}_h, \vec{\mathbf{u}}_h)\|_{\mathcal{H}_1 \times \mathcal{H}_2 \times \mathcal{Q}} \leqslant C_{\mathbf{T},\mathtt{d}} \Big\{ \rho \|\mathbf{z}_h\|^2_{0,4;\Omega} + \|\mathbf{u}_D\|_{1/2,\Gamma} + \|\mathbf{f}\|_{0,4/3;\Omega} \Big\} . \tag{5.13}$$

Proof. Thanks to the discrete inf-sup conditions for $\mathcal{B}$ (cf. (**H.7**)) and $\mathcal{B}_1$ (cf. (5.9)), and the properties (5.10), (5.11) and (5.12), the proof follows from a direct application of Theorem 4.1. We omit further details. □

Knowing that the discrete operator $\mathbf{T}_h$ is well defined, we now address the solvability of the fixed point equation (5.5). In fact, letting $\delta_{\mathtt{d}}$ be an arbitrary radius, we now set

$$\mathrm{W}(\delta_{\mathtt{d}}) := \Big\{ \mathbf{z}_h \in \mathcal{Q}_{1,h} : \quad \|\mathbf{z}_h\|_{0,4;\Omega} \leqslant \delta_{\mathtt{d}} \Big\} \quad \text{and} \quad \mathrm{S}(\delta_{\mathtt{d}}) := \mathrm{W}(\delta_{\mathtt{d}}) \times \mathcal{P}_h . \tag{5.14}$$

In this way, proceeding analogously to the deduction of Lemma 4.6, we find that, under the discrete analogue of (4.17), that is

$$\rho\, \delta_{\mathtt{d}} \leqslant \frac{1}{2\, C_{\mathbf{T},d}} \quad \text{and} \quad C_{\mathbf{T},\mathtt{d}} \Big\{ \|\mathbf{u}_D\|_{1/2,\Gamma} + \|\mathbf{f}\|_{0,4/3;\Omega} \Big\} \leqslant \frac{\delta_{\mathtt{d}}}{2} , \tag{5.15}$$

$\mathbf{T}_h$ maps $\mathrm{S}(\delta_{\mathtt{d}})$ into itself. Note that the above is the same as for the continuous case (cf. (4.17)), except that the constant $C_{\mathbf{T}}$ and the radius δ are replaced by $C_{\mathbf{T},\mathtt{d}}$ and $\delta_{\mathtt{d}}$, respectively.

In addition, employing similar arguments to those from the proof of Lemma 4.7, we can prove the discrete version of (4.18) with the constants

$$L_{1,\mathtt{d}}(\mathbf{T}) \,:=\, 2\,\big(1+2\,C_{\mathbf{T},\mathtt{d}}^{-1}\big)\,\alpha_{\mathcal{A}}^{-1}\,\widetilde{\beta}_{\mathtt{d}}^{-1}\,n^{1/2} \,+\, 2\,\big(1+L_{\mathcal{A}}\,\alpha_{\mathcal{A}}^{-1}\big)\,\widetilde{\beta}_{1,\mathtt{d}}^{-1}$$

and

$$L_{2,\mathtt{d}}(\mathbf{T}) \,:=\, \big(1+2\,C_{\mathbf{T},\mathtt{d}}^{-1}\big)\,\alpha_{\mathcal{A}}^{-1}\,\widetilde{\beta}_{\mathtt{d}}^{-1} \,+\, \big(1+L_{\mathcal{A}}\,\alpha_{\mathcal{A}}^{-1}\big)\,\widetilde{\beta}_{1,\mathtt{d}}^{-1}\,n^{-1/2}\,,$$

that is

$$\|\mathbf{T}_h(\mathbf{z}_h,r_h)-\mathbf{T}_h(\underset{\sim}{\mathbf{z}}_h,\underset{\sim}{r}_h)\| \,\leqslant\, L_{1,\mathtt{d}}(\mathbf{T})\,\rho\,\delta_{\mathtt{d}}\,\|\mathbf{z}_h-\underset{\sim}{\mathbf{z}}_h\|_{0,4;\Omega} \,+\, L_{2,\mathtt{d}}(\mathbf{T})\,L_\eta\,\|r_h-\underset{\sim}{r}_h\|_{0,\Omega} \tag{5.16}$$

for all $(\mathbf{z}_h,r_h),\ (\underset{\sim}{\mathbf{z}}_h,\underset{\sim}{r}_h)\in\mathrm{S}(\delta_{\mathtt{d}})$.

The main result of this section, which constitutes the discrete analogue of Theorem 4.8, is then established as follows.

Theorem 5.2. *Assume that $\rho\,\delta_{\mathtt{d}}$, L_η, and the data are sufficiently small so that*

$$\begin{gathered}\rho\,\delta_{\mathtt{d}} \,<\, \min\Big\{\frac{1}{2\,C_{\mathbf{T},\mathtt{d}}},\frac{1}{L_{1,\mathtt{d}}(\mathbf{T})}\Big\}\,, \qquad L_\eta \,<\, \frac{1}{L_{2,\mathtt{d}}(\mathbf{T})}\,, \quad \textit{and} \\ C_{\mathbf{T},\mathtt{d}}\,\Big\{\|\mathbf{u}_D\|_{1/2,\Gamma}+\|\mathbf{f}\|_{0,4/3;\Omega}\Big\} \,\leqslant\, \frac{\delta_{\mathtt{d}}}{2}\,.\end{gathered} \tag{5.17}$$

Then, the operator $\mathbf{T}_h$ has a unique fixed point $(\mathbf{u}_h,p_h)\in\mathrm{S}(\delta_{\mathtt{d}})$. Equivalently, given this $p_h\in\mathcal{P}_h$, the system (5.1) has a unique solution $(\mathbf{D}_h,\boldsymbol{\sigma}_h,\vec{\mathbf{u}}_h) \,:=\, \big(\mathbf{D}_h,\boldsymbol{\sigma}_h,(\mathbf{u}_h,\boldsymbol{\gamma}_h)\big)\in\mathcal{H}_{1,h}\times\mathcal{H}_{2,h}\times\mathcal{Q}_h$ with $\mathbf{u}_h\in\mathrm{W}(\delta_{\mathtt{d}})$ and p_h satisfying (5.4). Moreover, there holds

$$\|(\mathbf{D}_h,\boldsymbol{\sigma}_h,\vec{\mathbf{u}}_h)\|_{\mathcal{H}_1\times\mathcal{H}_2\times\mathcal{Q}} \,\leqslant\, 2\,C_{\mathbf{T},\mathtt{d}}\,\Big\{\|\mathbf{u}_D\|_{1/2,\Gamma} \,+\, \|\mathbf{f}\|_{0,4/3;\Omega}\Big\}\,. \tag{5.18}$$

Proof. It is clear from the previous discussion and the assumptions in (5.17), that $\mathbf{T}_h$ is a contraction mapping $\mathrm{S}(\delta_{\mathtt{d}})$ into itself. Thus, a straightforward application of the classical Banach Theorem implies the existence of a unique solution to (5.5), and hence, equivalently, to the system (5.1). In turn, thanks to (5.13) (cf. Theorem 5.1), and performing similar algebraic manipulations to those utilized in the proof of Theorem 4.8, we deduce the a priori estimate (5.18). □

5.3 A priori error analysis

In this section we consider arbitrary finite element subspaces satisfying the assumptions specified in Section 5.2, and derive the Céa estimate for the Galerkin error given by

$$\|\vec{\mathbf{D}}-\vec{\mathbf{D}}_h\|_{\mathcal{H}}+\|p-p_h\|_{0,\Omega} \,:=\, \|\mathbf{D}-\mathbf{D}_h\|_{0,\Omega} \,+\, \|\boldsymbol{\sigma}-\boldsymbol{\sigma}_h\|_{\mathbf{div}_{4/3};\Omega} \,+\, \|\vec{\mathbf{u}}-\vec{\mathbf{u}}_h\|_{\mathcal{Q}} \,+\, \|p-p_h\|_{0,\Omega}\,,$$

where $\vec{\mathbf{D}} \,:=\, (\mathbf{D},\boldsymbol{\sigma},\vec{\mathbf{u}}) \,=\, \big(\mathbf{D},\boldsymbol{\sigma},(\mathbf{u},\boldsymbol{\gamma})\big)\in\mathcal{H} \,:=\, \mathcal{H}_1\times\mathcal{H}_2\times\mathbf{Q}$ is the unique solution of (3.15), with $\mathbf{u}\in\mathrm{S}(\delta)$, and $\vec{\mathbf{D}}_h \,:=\, (\mathbf{D}_h,\boldsymbol{\sigma}_h,\vec{\mathbf{u}}_h) \,=\, \big(\mathbf{D}_h,\boldsymbol{\sigma}_h,(\mathbf{u}_h,\boldsymbol{\gamma}_h)\big)\in\mathcal{H}_h \,:=\, \mathcal{H}_{1,h}\times\mathcal{H}_{2,h}\times\mathbf{Q}_h$ is the unique solution of (5.1), with $\mathbf{u}_h\in\mathrm{S}(\delta_{\mathtt{d}})$, whereas p and p_h are computed according to (4.3) and (5.4), respectively.

We begin by defining for each $r \in \mathrm{L}^2_\kappa(\Omega)$ the operator $\boldsymbol{\Xi}_r : \mathcal{H} \to \mathcal{H}'$ that arises from the left-hand side of the variational formulation (3.15) after adding all its rows, that is

$$[\boldsymbol{\Xi}_r(\vec{\mathbf{C}}), \vec{\mathbf{E}}] \,:=\, [\mathcal{A}_r(\mathbf{C}), \mathbf{E}] \,+\, \mathcal{B}_1(\mathbf{E}, \boldsymbol{\zeta}) \,+\, \mathcal{B}_1(\mathbf{C}, \boldsymbol{\tau}) \,+\, \mathcal{B}(\boldsymbol{\tau}, \vec{\mathbf{w}}) \,+\, \mathcal{B}(\boldsymbol{\zeta}, \vec{\mathbf{v}})\,, \tag{5.19}$$

for all $\vec{\mathbf{C}} := (\mathbf{C}, \boldsymbol{\zeta}, \vec{\mathbf{w}})$, $\vec{\mathbf{E}} := (\mathbf{E}, \boldsymbol{\tau}, \vec{\mathbf{v}}) \in \mathcal{H}$, so that (3.15) and (5.1) can be rewritten, respectively, as

$$[\boldsymbol{\Xi}_p(\vec{\mathbf{D}}), \vec{\mathbf{E}}] \,=\, \mathcal{F}_{\mathbf{u}}(\mathbf{E}) + \mathcal{G}(\boldsymbol{\tau}) + \mathcal{F}(\vec{\mathbf{v}}) \qquad \forall\, \vec{\mathbf{E}} := (\mathbf{E}, \boldsymbol{\tau}, \vec{\mathbf{v}}) \in \mathcal{H}\,, \tag{5.20}$$

and

$$[\boldsymbol{\Xi}_{p_h}(\vec{\mathbf{D}}_h), \vec{\mathbf{E}}_h] \,=\, \mathcal{F}_{\mathbf{u}_h}(\mathbf{E}_h) + \mathcal{G}(\boldsymbol{\tau}_h) + \mathcal{F}(\vec{\mathbf{v}}_h) \qquad \forall\, \vec{\mathbf{E}}_h := (\mathbf{E}_h, \boldsymbol{\tau}_h, \vec{\mathbf{v}}_h) \in \mathcal{H}_h\,. \tag{5.21}$$

It readily follows from (5.20) and (5.21) that

$$[\boldsymbol{\Xi}_p(\vec{\mathbf{D}}), \vec{\mathbf{E}}_h] - [\boldsymbol{\Xi}_{p_h}(\vec{\mathbf{D}}_h), \vec{\mathbf{E}}_h] \,=\, \big(\mathcal{F}_{\mathbf{u}} - \mathcal{F}_{\mathbf{u}_h}\big)(\mathbf{E}_h) \qquad \forall\, \vec{\mathbf{E}}_h := (\mathbf{E}_h, \boldsymbol{\tau}_h, \vec{\mathbf{v}}_h) \in \mathcal{H}_h\,. \tag{5.22}$$

Now, the smoothness of the regularized η (cf. (2.11)) allows to show that for each $r \in \mathrm{L}^2_\kappa(\Omega)$, the operator $\mathcal{A}_r$, and hence $\boldsymbol{\Xi}_r$ as well, have first order Gâteaux derivatives $\mathcal{D}(\mathcal{A}_r) \in \mathcal{L}\big(\mathcal{H}_1, \mathcal{L}(\mathcal{H}_1, \mathcal{H}_1')\big)$ and $\mathcal{D}(\boldsymbol{\Xi}_r) \in \mathcal{L}\big(\mathcal{H}, \mathcal{L}(\mathcal{H}, \mathcal{H}')\big)$, respectively, as well as their corresponding discrete versions denoted by $\mathcal{D}_h(\mathcal{A}_r) \in \mathcal{L}\big(\mathcal{H}_{1,h}, \mathcal{L}(\mathcal{H}_{1,h}, \mathcal{H}_{1,h}')\big)$ and $\mathcal{D}_h(\boldsymbol{\Xi}_r) \in \mathcal{L}\big(\mathcal{H}_h, \mathcal{L}(\mathcal{H}_h, \mathcal{H}_h')\big)$. Moreover, using (4.9) and (4.10) (cf. Lemma 4.2), one is able to prove (see, e.g. [23, Lemma 3.1]) that for each $\mathbf{C}_h \in \mathcal{H}_{1,h}$, the operator $\mathcal{D}_h(\mathcal{A}_r)(\mathbf{C}_h) \in \mathcal{L}(\mathcal{H}_{1,h}, \mathcal{H}_{1,h}')$ can be identified as a bounded and $\mathcal{H}_1$-elliptic bilinear form with constants $L_{\mathcal{A}}$ and $\alpha_{\mathcal{A}}$, respectively. It follows that for each $r \in \mathrm{L}^2_\kappa(\Omega)$, and for each $\vec{\mathbf{C}}_h \in \mathcal{H}_h$, the operator $\mathcal{D}_h(\boldsymbol{\Xi}_r)(\vec{\mathbf{C}}_h) \in \mathcal{L}(\mathcal{H}_h, \mathcal{H}_h')$ satisfies the hypotheses of the discrete linear version of Theorem 4.1, and hence the corresponding global inf-sup condition as well with a positive constant $\alpha_{\boldsymbol{\Xi},\mathtt{d}}$, depending only on $\mathrm{L}_{\mathcal{A}}$, $\alpha_{\mathcal{A}}$, $\widetilde{\beta}_{\mathtt{d}}$, and $\widetilde{\beta}_{1,\mathtt{d}}$. In this way, proceeding analogously to the proof of [23, Theorem 3.3], which includes, in particular, applying the mean value theorem to $\boldsymbol{\Xi}_r$, we deduce that for each $r \in \mathrm{L}^2_\kappa(\Omega)$ there holds

$$\alpha_{\boldsymbol{\Xi},\mathtt{d}}\, \|\vec{\underset{\sim}{\mathbf{C}}}_h - \vec{\mathbf{C}}_h\|_{\mathcal{H}} \,\leqslant\, \sup_{\substack{\vec{\mathbf{E}}_h \in \mathcal{H}_h \\ \vec{\mathbf{E}}_h \neq \mathbf{0}}} \frac{[\boldsymbol{\Xi}_r(\vec{\underset{\sim}{\mathbf{C}}}_h) - \boldsymbol{\Xi}_r(\vec{\mathbf{C}}_h), \vec{\mathbf{E}}_h]}{\|\vec{\mathbf{E}}_h\|_{\mathcal{H}}} \qquad \forall\, \vec{\underset{\sim}{\mathbf{C}}}_h,\, \vec{\mathbf{C}}_h \in \mathcal{H}_h\,. \tag{5.23}$$

Then, we begin our derivation by employing the triangle inequality, which gives

$$\|\vec{\mathbf{D}} - \vec{\mathbf{D}}_h\|_{\mathcal{H}} \,\leqslant\, \|\vec{\mathbf{D}} - \vec{\mathbf{C}}_h\|_{\mathcal{H}} \,+\, \|\vec{\mathbf{D}}_h - \vec{\mathbf{C}}_h\|_{\mathcal{H}} \qquad \forall\, \vec{\mathbf{C}}_h \in \mathcal{H}_h\,, \tag{5.24}$$

whereas, applying (5.23) with $r = p$, we obtain

$$\alpha_{\boldsymbol{\Xi},\mathtt{d}}\, \|\vec{\mathbf{D}}_h - \vec{\mathbf{C}}_h\|_{\mathcal{H}} \,\leqslant\, \sup_{\substack{\vec{\mathbf{E}}_h \in \mathcal{H}_h \\ \vec{\mathbf{E}}_h \neq \mathbf{0}}} \frac{[\boldsymbol{\Xi}_p(\vec{\mathbf{D}}_h) - \boldsymbol{\Xi}_p(\vec{\mathbf{C}}_h), \vec{\mathbf{E}}_h]}{\|\vec{\mathbf{E}}_h\|_{\mathcal{H}}}\,. \tag{5.25}$$

Next, subtracting and adding $[\boldsymbol{\Xi}_p(\vec{\mathbf{D}}), \vec{\mathbf{E}}_h]$, we find that

$$[\boldsymbol{\Xi}_p(\vec{\mathbf{D}}_h) - \boldsymbol{\Xi}_p(\vec{\mathbf{C}}_h), \vec{\mathbf{E}}_h] \,=\, [\boldsymbol{\Xi}_p(\vec{\mathbf{D}}_h) - \boldsymbol{\Xi}_p(\vec{\mathbf{D}}), \vec{\mathbf{E}}_h] \,+\, [\boldsymbol{\Xi}_p(\vec{\mathbf{D}}) - \boldsymbol{\Xi}_p(\vec{\mathbf{C}}_h), \vec{\mathbf{E}}_h]\,, \tag{5.26}$$

so that, employing the Lipschitz-continuity of $\mathcal{A}_p$ (cf. (4.9), Lemma 4.2), we deduce from (5.19) the existence of a positive constant $L_{\boldsymbol{\Xi}}$, depending on $L_{\mathcal{A}}$, $\|\mathcal{B}\|$, and $\|\mathcal{B}_1\|$, such that the second term on the right-hand side of (5.26) is bounded as

$$\big|[\boldsymbol{\Xi}_p(\vec{\mathbf{D}}) - \boldsymbol{\Xi}_p(\vec{\mathbf{C}}_h), \vec{\mathbf{E}}_h]\big| \,\leqslant\, L_{\boldsymbol{\Xi}}\, \|\vec{\mathbf{D}} - \vec{\mathbf{C}}_h\|_{\mathcal{H}}\, \|\vec{\mathbf{E}}_h\|_{\mathcal{H}}\,. \tag{5.27}$$

In turn, subtracting and adding $[\boldsymbol{\Xi}_{p_h}(\vec{\mathbf{D}}_h),\vec{\mathbf{E}}_h]$, applying the Lipschitz-continuity of $\mathcal{A}$ with respect to the pressure (cf. (4.11), Lemma 4.2), and employing (5.22), we find that

$$\begin{aligned}\big|[\boldsymbol{\Xi}_p(\vec{\mathbf{D}}_h)-\boldsymbol{\Xi}_p(\vec{\mathbf{D}}),\vec{\mathbf{E}}_h]\big| &= \big|[\boldsymbol{\Xi}_p(\vec{\mathbf{D}}_h)-\boldsymbol{\Xi}_{p_h}(\vec{\mathbf{D}}_h),\vec{\mathbf{E}}_h]+[\boldsymbol{\Xi}_{p_h}(\vec{\mathbf{D}}_h)-\boldsymbol{\Xi}_p(\vec{\mathbf{D}}),\vec{\mathbf{E}}_h]\big| \\ &\leqslant \Big\{L_\eta\,\|p-p_h\|_{0,\Omega}\,+\,\|\mathcal{F}_{\mathbf{u}}-\mathcal{F}_{\mathbf{u}_h}\|_{\mathcal{H}'_{1,h}}\Big\}\,\|\vec{\mathbf{E}}_h\|_{\mathcal{H}}\,.\end{aligned} \tag{5.28}$$

In this way, using (5.27) and (5.28) to bound the expression in (5.26), and then replacing the resulting estimate in (5.25), we arrive at

$$\alpha_{\boldsymbol{\Xi},\mathtt{d}}\,\|\vec{\mathbf{D}}_h-\vec{\mathbf{C}}_h\|_{\mathcal{H}}\,\leqslant\,L_{\boldsymbol{\Xi}}\,\|\vec{\mathbf{D}}-\vec{\mathbf{C}}_h\|_{\mathcal{H}}+L_\eta\,\|p-p_h\|_{0,\Omega}\,+\,\|\mathcal{F}_{\mathbf{u}}-\mathcal{F}_{\mathbf{u}_h}\|_{\mathcal{H}'_{1,h}}\,, \tag{5.29}$$

which, along with (5.24), implies

$$\|\vec{\mathbf{D}}-\vec{\mathbf{D}}_h\|_{\mathcal{H}}\,\leqslant\,\big(1+\alpha^{-1}_{\boldsymbol{\Xi},\mathtt{d}}\,L_{\boldsymbol{\Xi}}\big)\,\mathrm{dist}(\vec{\mathbf{D}},\mathcal{H}_h\big)+\alpha^{-1}_{\boldsymbol{\Xi},\mathtt{d}}\,\Big\{L_\eta\,\|p-p_h\|_{0,\Omega}\,+\,\|\mathcal{F}_{\mathbf{u}}-\mathcal{F}_{\mathbf{u}_h}\|_{\mathcal{H}'_{1,h}}\Big\}\,, \tag{5.30}$$

where, as usual,

$$\mathrm{dist}(\vec{\mathbf{D}},\mathcal{H}_h\big)\,:=\,\inf_{\vec{\mathbf{C}}_h\in\mathcal{H}_h}\|\vec{\mathbf{D}}-\vec{\mathbf{C}}_h\|_{\mathcal{H}}\,.$$

Furthermore, according to the expressions provided by (4.3) and (5.4), and proceeding similarly to the derivation of the last two terms in (4.32), we get

$$\|p-p_h\|_{0,\Omega}\,\leqslant\,n^{-1/2}\,\Big\{\|\boldsymbol{\sigma}-\boldsymbol{\sigma}_h\|_{0,\Omega}\,+\,2\,\rho\,\|(\mathbf{u}\otimes\mathbf{u})-(\mathbf{u}_h\otimes\mathbf{u}_h)\|_{0,\Omega}\Big\}\,. \tag{5.31}$$

In addition, invoking now the definition of $\mathcal{F}_{\mathbf{z}}$ (cf. (3.19)) as in (4.23), we obtain

$$\big(\mathcal{F}_{\mathbf{u}}-\mathcal{F}_{\mathbf{u}_h}\big)(\mathbf{E}_h)\,=\,\rho\int_\Omega\big((\mathbf{u}\otimes\mathbf{u})-(\mathbf{u}_h\otimes\mathbf{u}_h)\big):\mathbf{E}_h\qquad\forall\,\mathbf{E}_h\in\mathcal{H}_{1,h}\,,$$

which gives

$$\|\mathcal{F}_{\mathbf{u}}-\mathcal{F}_{\mathbf{u}_h}\|_{\mathcal{H}'_{1,h}}\,\leqslant\,\rho\,\|(\mathbf{u}\otimes\mathbf{u})-(\mathbf{u}_h\otimes\mathbf{u}_h)\|_{0,\Omega}\,. \tag{5.32}$$

Then, replacing the bounds from (5.31) and (5.32) back into (5.30), and denoting the constants

$$C_{1,\boldsymbol{\Xi}}\,:=\,1+\alpha^{-1}_{\boldsymbol{\Xi},\mathtt{d}}\,L_{\boldsymbol{\Xi}}\,,\quad C_{2,\boldsymbol{\Xi}}\,:=\,\alpha^{-1}_{\boldsymbol{\Xi},\mathtt{d}}\,n^{-1/2}\,,\quad\text{and}\quad C_{3,\boldsymbol{\Xi}}\,:=\,\alpha^{-1}_{\boldsymbol{\Xi},\mathtt{d}}\,\rho\,\big(2\,n^{-1/2}\,L_\eta+1\big)\,,$$

we conclude that

$$\|\vec{\mathbf{D}}-\vec{\mathbf{D}}_h\|_{\mathcal{H}}\,\leqslant\,C_{1,\boldsymbol{\Xi}}\,\mathrm{dist}(\vec{\mathbf{D}},\mathcal{H}_h\big)+C_{2,\boldsymbol{\Xi}}\,L_\eta\,\|\boldsymbol{\sigma}-\boldsymbol{\sigma}_h\|_{0,\Omega}+C_{3,\boldsymbol{\Xi}}\,\|(\mathbf{u}\otimes\mathbf{u})-(\mathbf{u}_h\otimes\mathbf{u}_h)\|_{0,\Omega}\,. \tag{5.33}$$

Finally, similarly to the derivation of (4.24), there holds

$$\|(\mathbf{u}\otimes\mathbf{u})-(\mathbf{u}_h\otimes\mathbf{u}_h)\|_{0,\Omega}\,\leqslant\,n^{1/2}\,\big(\|\mathbf{u}\|_{0,4;\Omega}+\|\mathbf{u}_h\|_{0,4;\Omega}\big)\,\|\mathbf{u}-\mathbf{u}_h\|_{0,4;\Omega}\,\leqslant\,n^{1/2}\,\big(\delta+\delta_{\mathtt{d}}\big)\,\|\mathbf{u}-\mathbf{u}_h\|_{0,4;\Omega}\,, \tag{5.34}$$

and hence the inequalities (5.31) and (5.33) become, respectively,

$$\|p-p_h\|_{0,\Omega}\,\leqslant\,n^{-1/2}\,\|\boldsymbol{\sigma}-\boldsymbol{\sigma}_h\|_{0,\Omega}\,+\,2\,\rho\,\big(\delta+\delta_{\mathtt{d}}\big)\,\|\mathbf{u}-\mathbf{u}_h\|_{0,4;\Omega}\,, \tag{5.35}$$

and

$$\|\vec{\mathbf{D}}-\vec{\mathbf{D}}_h\|_{\mathcal{H}}\,\leqslant\,C_{1,\boldsymbol{\Xi}}\,\mathrm{dist}(\vec{\mathbf{D}},\mathcal{H}_h\big)+C_{2,\boldsymbol{\Xi}}\,L_\eta\,\|\boldsymbol{\sigma}-\boldsymbol{\sigma}_h\|_{0,\Omega}+C_{3,\boldsymbol{\Xi}}\,n^{1/2}\,\big(\delta+\delta_{\mathtt{d}}\big)\,\|\mathbf{u}-\mathbf{u}_h\|_{0,4;\Omega}\,. \tag{5.36}$$

We are now in position to establish the main result of this section.

Theorem 5.3. *In addition to the notations and hypotheses of Theorems* 4.8 *and* 5.2*, assume that* L_η*, and the radii* δ *and* δ_d *are sufficiently small so that*

$$C_{2,\boldsymbol{\Xi}}\, L_\eta \,\leqslant\, \frac{1}{2} \quad \textit{and} \quad C_{3,\boldsymbol{\Xi}}\, n^{1/2}\,\big(\delta + \delta_{\mathtt{d}}\big) \,\leqslant\, \frac{1}{2}\,. \tag{5.37}$$

Then, there exists a positive constant C*, independent of* h*, such that*

$$\|\vec{\mathbf{D}} - \vec{\mathbf{D}}_h\|_{\mathcal{H}} + \|p - p_h\|_{0,\Omega} \,\leqslant\, C\,\mathrm{dist}(\vec{\mathbf{D}}, \mathcal{H}_h)\,. \tag{5.38}$$

Proof. By employing (5.37) in (5.36), we readily deduce that

$$\|\vec{\mathbf{D}} - \vec{\mathbf{D}}_h\|_{\mathcal{H}} \,\leqslant\, 2\,C_{1,\boldsymbol{\Xi}}\,\mathrm{dist}(\vec{\mathbf{D}}, \mathcal{H}_h)\,,$$

whereas the corresponding estimate for $\|p-p_h\|_{0,\Omega}$ follows from (5.35) and the foregoing inequality. □

6 Specific finite element subspaces

In this section we proceed as in [24, Section 4.4], where, in turn, the analysis from [25, Section 4.4] is employed, to describe two examples of finite element subspaces $\mathcal{H}_{1,h}$, $\widetilde{\mathcal{H}}_{2,h}$, $\mathcal{Q}_{1,h}$, and $\mathcal{Q}_{2,h}$, satisfying the hypotheses (**H.4**), (**H.5**), (**H.6**), and (**H.7**) that were introduced in Section 5.2. The associated rates of convergence are also provided.

6.1 Polynomial spaces

We first collect some definitions regarding local and global polynomial spaces, for which we make use of the regular family of triangulations $\{\mathcal{T}_h\}_{h>0}$ of $\bar{\Omega}$ introduced in Section 5.1. Indeed, given an integer $\ell \geqslant 0$ and $K \in \mathcal{T}_h$, we let $\mathrm{P}_\ell(K)$ be the space of polynomials of degree $\leqslant \ell$ defined on K, and denote its vector and tensor versions by $\mathbf{P}_\ell(K) := [\mathrm{P}_\ell(K)]^n$ and $\mathbb{P}_\ell(K) = [\mathrm{P}_\ell(K)]^{n\times n}$, respectively. In addition, we let $\mathbb{RT}_\ell(K) := \mathbf{P}_\ell(K) \oplus \mathrm{P}_\ell(K)\,\mathbf{x}$ be the local Raviart–Thomas space of order ℓ defined on K, where $\mathbf{x}$ stands for a generic vector in $\mathbf{R} := \mathrm{R}^n$. Also, we let b_K be the bubble function on K, which is defined as the product of its $n+1$ barycentric coordinates. Then, we define the local bubble spaces of order ℓ as

$$\mathbf{B}_\ell(K) := \mathrm{curl}\,\big(b_K\,\mathrm{P}_\ell(K)\big) \quad \text{if} \quad n = 2\,, \quad \text{and} \quad \mathbf{B}_\ell(K) := \mathrm{curl}\,\big(b_K\,\mathbf{P}_\ell(K)\big) \quad \text{if} \quad n = 3\,, \tag{6.1}$$

where $\mathrm{curl}\,(v) := \big(\frac{\partial v}{\partial x_2}, -\frac{\partial v}{\partial x_1}\big)$ if $n = 2$ and $v : K \to \mathrm{R}$, and $\mathrm{curl}\,(\mathbf{v}) := \nabla \times \mathbf{v}$ if $n = 3$ and $\mathbf{v} : K \to \mathrm{R}^3$. The following global spaces are also needed

$$\mathbf{P}_\ell(\Omega) := \Big\{\mathbf{v}_h \in \mathbf{L}^2(\Omega) : \quad \mathbf{v}_h|_K \,\in\, \mathbf{P}_\ell(K) \quad \forall\, K \in \mathcal{T}_h\Big\}\,,$$

$$\mathbb{P}_\ell(\Omega) := \Big\{\boldsymbol{\xi}_h \in \mathbb{L}^2(\Omega) : \quad \boldsymbol{\xi}_h|_K \,\in\, \mathbb{P}_\ell(K) \quad \forall\, K \in \mathcal{T}_h\Big\}\,,$$

$$\mathbb{RT}_\ell(\Omega) := \Big\{\boldsymbol{\tau}_h \in \mathbb{H}(\mathbf{div};\Omega) : \quad \boldsymbol{\tau}_{h,i}|_K \,\in\, \mathbb{RT}_\ell(K) \quad \forall\, i \in \{1,...,n\}\,, \quad \forall\, K \in \mathcal{T}_h\Big\}\,,$$

and

$$\mathbb{B}_\ell(\Omega) := \Big\{\boldsymbol{\tau}_h \in \mathbb{H}(\mathbf{div};\Omega) : \quad \boldsymbol{\tau}_{h,i}|_K \,\in\, \mathbf{B}_\ell(K) \quad \forall\, i \in \{1,...,n\}\,, \quad \forall\, K \in \mathcal{T}_h\Big\}\,,$$

where $\boldsymbol{\tau}_{h,i}$ stands for the ith-row of $\boldsymbol{\tau}_h$. While $\mathbf{P}_\ell(\Omega)$ and $\mathbb{P}_\ell(\Omega)$ are defined here as subspaces of $\mathbf{L}^2(\Omega)$ and $\mathbb{L}^2(\Omega)$, we stress that they are also subspaces of $\mathbf{L}^4(\Omega)$ and $\mathbb{L}^4(\Omega)$, respectively. Similarly,

it is easy to see that $\mathbb{RT}_\ell(\Omega)$ and $\mathbb{B}_\ell(\Omega)$ are both subspaces of $\mathbb{H}(\mathbf{div}_{4/3};\Omega)$ as well. Actually, recalling that $\mathbb{H}(\mathbf{div};\Omega)$ stands for the Hilbertian version of (1.2), that is with $t=2$, it is clear that $\mathbb{H}(\mathbf{div};\Omega)$ is contained in $\mathbb{H}(\mathbf{div}_{4/3};\Omega)$, and hence any subspace of the former is also subspace of the latter. Certainly, the same observation is valid for $\mathbb{H}_0(\mathbf{div};\Omega)$ and $\mathbb{H}_0(\mathbf{div}_{4/3};\Omega)$, where the former is defined analogously to (3.11).

6.2 Connection with linear elasticity

Here we describe a useful connection between (**H.7**) and the stability of a usual mixed finite element method for the linear elasticity model. We begin by recalling that a triplet of subspaces $\widetilde{\mathcal{H}}_{2,h}$, $\mathcal{Q}_{1,h}$, and $\mathcal{Q}_{2,h}$ of $\mathbb{H}(\mathbf{div};\Omega)$, $\mathbf{L}^2(\Omega)$, and $\mathbb{L}^2_{\mathtt{sk}}(\Omega)$, respectively, is said to yield a stable Galerkin scheme for the Hilbertian mixed formulation of linear elasticity if it satisfies the corresponding hypotheses of the discrete Babuška-Brezzi theory (see, e.g., [22, Theorem 2.4]). In particular, the above includes the discrete inf-sup condition for the bilinear form $\mathcal{B}$ (cf. (3.18)), which, setting $\mathcal{H}_{2,h} := \widetilde{\mathcal{H}}_{2,h} \cap \mathbb{H}_0(\mathbf{div};\Omega)$, reduces to the existence of a positive constant $\widetilde{\beta}_{\mathtt{e}}$, independent of h, such that

$$\sup_{\substack{\boldsymbol{\tau}_h \in \mathcal{H}_{2,h} \\ \boldsymbol{\tau}_h \neq 0}} \frac{\mathcal{B}(\boldsymbol{\tau}_h, \vec{\mathbf{v}}_h)}{\|\boldsymbol{\tau}_h\|_{\mathbf{div};\Omega}} \geqslant \widetilde{\beta}_{\mathtt{e}} \Big\{ \|\mathbf{v}_h\|_{0,\Omega} + \|\boldsymbol{\xi}_h\|_{0,\Omega} \Big\} \qquad \forall\, \vec{\mathbf{v}}_h := (\mathbf{v}_h, \boldsymbol{\xi}_h) \in \mathcal{Q}_h \,. \tag{6.2}$$

Note that, though similar, (6.2) and (5.7) differ because of the different norms in which $\boldsymbol{\tau}_h$ and $\mathbf{v}_h$ are measured. However, the following result (cf. [25, Lemma 4.8]) establishes that (6.2), along with suitable further assumptions on the subspaces, constitute a sufficient condition for (5.7).

Lemma 6.1. *Let $\widetilde{\mathcal{H}}_{2,h}$, $\mathcal{Q}_{1,h}$, and $\mathcal{Q}_{2,h}$ be subspaces of $\mathbb{H}(\mathbf{div};\Omega)$, $\mathbf{L}^2(\Omega)$, and $\mathbb{L}^2_{\mathtt{sk}}(\Omega)$, respectively, such that they accomplish (6.2). In addition, assume that there exists an integer $\ell \geqslant 0$ such that $\mathbb{RT}_\ell(\Omega) \subseteq \widetilde{\mathcal{H}}_{2,h}$ and $\mathcal{Q}_{1,h} \subseteq \mathbf{P}_\ell(\Omega)$. Then $\mathcal{H}_{2,h} := \widetilde{\mathcal{H}}_{2,h} \cap \mathbb{H}_0(\mathbf{div}_{4/3};\Omega)$, $\mathcal{Q}_{1,h}$, and $\mathcal{Q}_{2,h}$ satisfy (5.7) with a positive constant $\widetilde{\beta}_{\mathtt{d}}$, independent of h.*

6.3 Examples of stable finite element subspaces

We now apply Lemma 6.1 to each one of the stable triplets for linear elasticity proposed in [25, Section 4.4], thus deriving two examples of finite element subspaces $\mathcal{H}_{1,h}$, $\widetilde{\mathcal{H}}_{2,h}$, $\mathcal{Q}_{1,h}$, and $\mathcal{Q}_{2,h}$ satisfying (**H.4**), (**H.5**), (**H.6**), and (**H.7**).

Our first example is based on the plane elasticity element with reduced symmetry (PEERS) of order $\ell \geqslant 0$, which, denoting $\mathbb{C}(\bar{\Omega}) := [C(\bar{\Omega})]^{n\times n}$, is given by

$$\widetilde{\mathcal{H}}_{2,h} := \mathbb{RT}_\ell(\Omega) \oplus \mathbb{B}_\ell(\Omega)\,, \quad \mathcal{Q}_{1,h} := \mathbf{P}_\ell(\Omega)\,, \quad \text{and} \quad \mathcal{Q}_{2,h} := \mathbb{C}(\bar{\Omega}) \cap \mathbb{P}_{\ell+1}(\Omega) \cap \mathbb{L}^2_{\mathtt{sk}}(\Omega)\,. \tag{6.3}$$

The discrete stability of these subspaces was originally proved in [3] for $\ell = 0$ and $n = 2$, and later on for $\ell \geqslant 0$ and $n \in \{2,3\}$ in [34]. It is easily seen from (6.3), in particular using due to (6.1) that $\mathbf{div}(\widetilde{\mathcal{H}}_{2,h}) = \mathbf{div}\big(\mathbb{RT}_\ell(\Omega)\big) \subseteq \mathbf{P}_\ell(\Omega)$, that $\widetilde{\mathcal{H}}_{2,h}$ and $\mathcal{Q}_{1,h}$ satisfy (**H.4**) and (**H.5**), and that the assumptions on them required by Lemma 6.1 are accomplished as well, whence (**H.7**) holds true. It remains to check (**H.6**), for which we first recall that the divergence free tensors of $\mathbb{RT}_\ell(\Omega)$ are contained in $\mathbb{P}_\ell(\Omega)$ (cf. [22, proof of Theorem 3.3]). Thus, noting again that the tensors of $\mathbb{B}_\ell(\Omega)$ are divergence free, and that this space is contained in $\mathbb{P}_{\ell+n}(\Omega)$, we deduce from (5.8) that

$$\mathcal{V}_h \subseteq \mathbb{P}_\ell(\Omega) \oplus \mathbb{B}_\ell(\Omega) \subseteq \mathbb{P}_{\ell+n}(\Omega)\,,$$

so that, in order to guarantee (**H.6**), it suffices to take

$$\mathcal{H}_{1,h} \,:=\, \mathbb{P}_{\ell+n}(\Omega) \,\cap\, \mathbb{L}^2_{\mathtt{tr}}(\Omega)\,.$$

Finally, it follows from (5.4) and the above definitions of $\mathcal{H}_{2,h}$ and $\mathcal{Q}_{1,h}$, that $\mathcal{P}_h := \widetilde{\mathcal{P}}_h \oplus \Big\{ \dfrac{\kappa}{|\Omega|} \Big\}$, where $\widetilde{\mathcal{P}}_h \,:=\, \mathrm{P}_{\bar{\ell}}(\Omega) \,\cap\, \mathrm{L}^2_0(\Omega)$, with $\bar{\ell} \,:=\, \max\big\{\ell+n, 2\,\ell\big\}$. Our second example is the Arnold-Falk-Winther (AFW) element of order $\ell \geqslant 0$, whose stability for the Hilbertian mixed formulation of linear elasticity is proved in [4], and which is defined as

$$\widetilde{\mathcal{H}}_{2,h} \,:=\, \mathbb{P}_{\ell+1}(\Omega) \cap \mathbb{H}(\mathbf{div};\Omega)\,, \quad \mathcal{Q}_{1,h} \,:=\, \mathbf{P}_{\ell}(\Omega)\,, \quad \text{and} \quad \mathcal{Q}_{2,h} \,:=\, \mathbb{P}_{\ell}(\Omega) \cap \mathbb{L}^2_{\mathtt{sk}}(\Omega)\,. \tag{6.4}$$

According to the above, it is also simple to realize that (**H.4**) and (**H.5**) are satisfied, and that, thanks to the inclusion $\mathbb{RT}_{\ell}(\Omega) \subseteq \mathbb{P}_{\ell+1}(\Omega)$, the corresponding hypotheses of Lemma 6.1 are fulfilled, thus establishing (**H.7**). In turn, being in this case $\mathcal{V}_h$ (cf. (5.8)) not further simplifiable, we deduce that (**H.6**) is accomplished if we simply choose

$$\mathcal{H}_{1,h} \,:=\, \mathbb{P}_{\ell+1}(\Omega) \,\cap\, \mathbb{L}^2_{\mathtt{tr}}(\Omega)\,.$$

Furthermore, it is readily seen in this case that $\mathcal{P}_h := \widetilde{\mathcal{P}}_h \oplus \Big\{ \dfrac{\kappa}{|\Omega|} \Big\}$, where $\widetilde{\mathcal{P}}_h \,:=\, \mathrm{P}_{2\ell}(\Omega) \,\cap\, \mathrm{L}^2_0(\Omega)$.

6.4 The rates of convergence

We now provide the rates of convergence of (5.1) for both specific examples of finite element subspaces introduced in Section 6.3. To this end, we first collect next the corresponding approximation properties of $\mathcal{H}_{1,h}$, $\mathcal{H}_{2,h}$, $\mathcal{Q}_{1,h}$, and $\mathcal{Q}_{2,h}$, which, taken mainly from [8], [9], [16, eqs. (5.37) and (5.40)], and [20, Proposition 1.135], are derived by employing the error estimates of suitable interpolation and projection operators, along with associated commuting diagram properties and interpolation estimates of Sobolev spaces.

Denoting $\ell^* := \left\{ \begin{array}{ll} \ell+n & \text{for PEERS-based} \\ \ell+1 & \text{for AFW-based} \end{array} \right.$, the respective statements are as follows:

$\mathbf{AP}\big(\mathcal{H}_{1,h}\big)$ there exists a positive constant C, independent of h, such that for each $r \in [0, \ell^*+1]$, and for each $\mathbf{E} \in \mathbb{H}^r(\Omega) \cap \mathbb{L}^2_{\mathrm{tr}}(\Omega)$, there holds

$$\mathrm{dist}\big(\mathbf{E}, \mathcal{H}_{1,h}\big) \,:=\, \inf_{\mathbf{E}_h \in \mathcal{H}_{1,h}} \|\mathbf{E} - \mathbf{E}_h\|_{0,\Omega} \,\leqslant\, C\, h^r \|\mathbf{E}\|_{r,\Omega}\,,$$

$\mathbf{AP}\big(\mathcal{H}_{2,h}\big)$ there exists a positive constant C, independent of h, such that for each $r \in (0, \ell+1]$, and for each $\boldsymbol{\tau} \in \mathbb{H}^r(\Omega) \cap \mathbb{H}_0(\mathbf{div}_{4/3};\Omega)$ with $\mathbf{div}(\boldsymbol{\tau}) \in \mathbf{W}^{r,4/3}(\Omega)$, there holds

$$\mathrm{dist}\big(\boldsymbol{\tau}, \mathcal{H}_{2,h}\big) \,:=\, \inf_{\boldsymbol{\tau}_h \in \mathcal{H}_{2,h}} \|\boldsymbol{\tau} - \boldsymbol{\tau}_h\|_{\mathbf{div}_{4/3};\Omega} \,\leqslant\, C\, h^r \Big\{ \|\boldsymbol{\tau}\|_{r,\Omega} \,+\, \|\mathbf{div}(\boldsymbol{\tau})\|_{r,4/3;\Omega} \Big\}\,,$$

$\mathbf{AP}\big(\mathcal{Q}_{1,h}\big)$ there exists a positive constant C, independent of h, such that for each $r \in [0, \ell+1]$, and for each $\mathbf{v} \in \mathbf{W}^{r,4}(\Omega)$, there holds

$$\mathrm{dist}\big(\mathbf{v}, \mathcal{Q}_{1,h}\big) \,:=\, \inf_{\mathbf{v}_h \in \mathcal{Q}_{1,h}} \|\mathbf{v} - \mathbf{v}_h\|_{0,4;\Omega} \,\leqslant\, C\, h^r \|\mathbf{v}\|_{r,4;\Omega}\,,$$

$\mathbf{AP}\big(\mathcal{Q}_{2,h}\big)$ there exists a positive constant C, independent of h, such that for each $r \in [0, \ell+1]$, and for each $\boldsymbol{\xi} \in \mathbb{H}^r(\Omega) \cap \mathbb{L}^2_{\mathtt{sk}}(\Omega)$, there holds

$$\mathrm{dist}\big(\boldsymbol{\xi}, \mathcal{Q}_{2,h}\big) := \inf_{\boldsymbol{\xi}_h \in \mathcal{Q}_{2,h}} \|\boldsymbol{\xi} - \boldsymbol{\xi}_h\|_{0,\Omega} \leqslant C\, h^r \|\boldsymbol{\xi}\|_{r,\Omega}\,.$$

As a consequence of the Céa estimate (5.38) (cf. Theorem 5.3), along with $\mathbf{AP}\big(\mathcal{H}_{1,h}\big)$, $\mathbf{AP}\big(\mathcal{H}_{2,h}\big)$, $\mathbf{AP}\big(\mathcal{Q}_{1,h}\big)$, and $\mathbf{AP}\big(\mathcal{Q}_{2,h}\big)$, we are now able to provide the main result of this section.

Theorem 6.2. *In addition to the notations and hypotheses of Theorem* 5.3*, assume that there exists* $r \in (0, \ell+1]$*, such that* $\mathbf{D} \in \mathbb{H}^r(\Omega) \cap \mathbb{L}^2_{\mathrm{tr}}(\Omega)$*,* $\boldsymbol{\sigma} \in \mathbb{H}^r(\Omega) \cap \mathbb{H}_0(\mathbf{div}_{4/3}; \Omega)$*,* $\mathbf{div}(\boldsymbol{\sigma}) \in \mathbf{W}^{r,4/3}(\Omega)$*,* $\mathbf{u} \in \mathbf{W}^{r,4}(\Omega)$*, and* $\boldsymbol{\gamma} \in \mathbb{H}^r(\Omega) \cap \mathbb{L}^2_{\mathtt{sk}}(\Omega)$*. Then, there exists a positive constant* C*, independent of* h*, such that*

$$\|\vec{\mathbf{D}} - \vec{\mathbf{D}}_h\|_{\mathcal{H}} + \|p - p_h\|_{0,\Omega} \leqslant C\, h^r \Big\{ \|\mathbf{D}\|_{r,\Omega} + \|\boldsymbol{\sigma}\|_{r,\Omega} + \|\mathbf{div}(\boldsymbol{\sigma})\|_{r,4/3;\Omega} + \|\mathbf{u}\|_{r,4;\Omega} + \|\boldsymbol{\gamma}\|_{r,\Omega} \Big\}\,.$$

7 Numerical results

In this section we consider the two pairs of finite element subspaces detailed in Section 6 to present three examples illustrating the performance of the mixed finite element method (5.1) on a set of quasi-uniform triangulations of the respective domains. In what follows, we refer to the corresponding sets of finite element subspaces generated by $\ell = \{0, 1\}$ as simply PEERS_ℓ and AFW_ℓ based discretizations. The numerical methods have been implemented using the open source finite element library `FEniCS` [1]. The corresponding iterative procedure to solve the nonlinear problem (5.1) is described as follows:

(1) Start solving the Stokes problem arising from (5.1) by choosing $\eta = 1$ and $\rho = 0$ to obtain the initial data: $(\mathbf{D}_h^0, \mathbf{u}_h^0) \in \mathcal{H}_{1,h} \times \mathcal{Q}_{1,h}$ and p_h^0 as in (5.4).

(2) Given $(\mathbf{D}_h^0, \mathbf{u}_h^0, p_h^0)$ from step (1), for each $m \geqslant 1$, a Newton-type strategy is used to obtain the solution of (5.1): $(\mathbf{D}_h^m, \boldsymbol{\sigma}_h^m, \vec{\mathbf{u}}_h^m) := \big(\mathbf{D}_h^m, \boldsymbol{\sigma}_h^m, (\mathbf{u}_h^m, \boldsymbol{\gamma}_h^m)\big) \in \mathcal{H}_{1,h} \times \mathcal{H}_{2,h} \times \mathcal{Q}_h$.

(3) Update the pressure p_h^m by employing the formula (5.4), and go to step (2).

The iterative method is finished when the relative error between two consecutive iterations of the complete coefficient vector, namely $\mathbf{coeff}^m$ and $\mathbf{coeff}^{m+1}$, is sufficiently small, that is,

$$\frac{\|\mathbf{coeff}^{m+1} - \mathbf{coeff}^m\|_{\mathtt{DOF}}}{\|\mathbf{coeff}^{m+1}\|_{\mathtt{DOF}}} \leqslant \mathsf{tol}\,,$$

where $\|\cdot\|_{\mathtt{DOF}}$ stands for the usual Euclidean norm in $\mathrm{R}^{\mathtt{DOF}}$ with `DOF` denoting the total number of degrees of freedom defining the finite element subspaces $\mathcal{H}_{1,h}$, $\widetilde{\mathcal{H}}_{2,h}$, $\mathcal{Q}_{1,h}$, and $\mathcal{Q}_{2,h}$ (cf. (6.3)–(6.4)), and tol is a fixed tolerance chosen as $\mathsf{tol} = 1E-06$.

We now introduce some additional notation. The individual errors are denoted by

$$\mathsf{e}(\mathbf{D}) := \|\mathbf{D} - \mathbf{D}_h\|_{0,\Omega}\,, \quad \mathsf{e}(\boldsymbol{\sigma}) := \|\boldsymbol{\sigma} - \boldsymbol{\sigma}_h\|_{\mathbf{div}_{4/3};\Omega}\,, \quad \mathsf{e}(\mathbf{u}) := \|\mathbf{u} - \mathbf{u}_h\|_{0,4;\Omega}\,,$$
$$\mathsf{e}(\boldsymbol{\gamma}) := \|\boldsymbol{\gamma} - \boldsymbol{\gamma}_h\|_{0,\Omega}\,, \quad \mathbf{e}(p) := \|p - p_h\|_{0,\Omega}\,,$$

and, as usual, for each $\star \in \big\{\mathbf{D}, \boldsymbol{\sigma}, \mathbf{u}, \boldsymbol{\gamma}, p\big\}$ we let $\mathsf{r}(\star)$ be the experimental rate of convergence given by $\mathsf{r}(\star) := \log(\mathsf{e}(\star)/\widehat{\mathsf{e}}(\star))/\log(h/\widehat{h})$, where h and $\widehat{h}$ denote two consecutive meshsizes with errors e and $\widehat{\mathsf{e}}$, respectively.

The examples to be considered in this section are described next, for which we consider the regularized viscosity $\eta(\varrho,\omega)$ defined by (2.11), but without needing to make use of the modification described by Figure A.1. In the first two examples, for the sake of simplicity, we take $\mu_s = 0.1$, $\mu_d = 1$, $I_0 = 1$, $d = 1$ and $\rho = 1$. In addition, the null mean value of $\mathrm{tr}(\boldsymbol{\sigma}_h)$ over Ω is fixed via a real Lagrange multiplier strategy.

Example 1: Convergence against smooth exact solutions in a 2D domain

In this test we corroborate the rates of convergence in a two-dimensional domain set by the square $\Omega = (0,1)^2$. We choose the regularization factor $\varepsilon = 1E-08$, and adjust the datum $\mathbf{f}$ in (2.19) such that the exact solution is given by

$$\mathbf{u}(x_1,x_2) \,=\, \begin{pmatrix} \sin(x_1)\cos(x_2) \\ -\cos(x_1)\sin(x_2) \end{pmatrix} \quad \text{and} \quad p(x_1,x_2) \,=\, \exp(x_1+x_2), \tag{7.1}$$

where $p \in \mathrm{L}^2_\kappa(\Omega)$, with $\kappa = (\exp(1)-1)^2$. The model problem is then complemented with the appropriate Dirichlet boundary condition. Tables 7.1 and 7.2 show the convergence history for a sequence of quasi-uniform mesh refinements, including the number of Newton iterations. As already announced, we stress that we are able not only to approximate the original unknowns but also the pressure field through the formula (5.4). The results confirm that the optimal rates of convergence $\mathcal{O}(h^{\ell+1})$ predicted by Theorem 6.2 are attained for $\ell = \{0,1\}$ for both PEERS$_\ell$ and AFW$_\ell$ based schemes. The Newton method exhibits a behavior dependent on the mesh size, converging faster for finer meshes in both discrete schemes. The latter is justified by the fact that for finer mesh a better initial data $(\mathbf{D}_h^0, \mathbf{u}_h^0)$ and p_h^0 are provided for the iterative method. In Figure 7.1 we display the discrete internal friction coefficient $\mu(I_h)$ recovered from (2.7), with $I_h = \sqrt{2}\,d\,|\mathbf{D}_h|/\sqrt{p_h/\rho}$, and some solutions obtained with the mixed PEERS$_1$ approximation with meshsize $h = 0.014$ and $20,000$ triangle elements (actually representing $1,081,202$ DOF).

PEERS$_\ell$–based discretization with $\ell = 0$												
DOF	h	it	e($\mathbf{D}$)	r($\mathbf{D}$)	e($\boldsymbol{\sigma}$)	r($\boldsymbol{\sigma}$)	e($\mathbf{u}$)	r($\mathbf{u}$)	e($\boldsymbol{\gamma}$)	r($\boldsymbol{\gamma}$)	e(p)	r(p)
842	0.354	16	3.15e-01	–	1.14e+00	–	7.84e-02	–	1.08e-01	–	4.27e-01	–
3314	0.177	14	1.87e-01	0.750	5.53e-01	1.044	3.70e-02	1.085	4.58e-02	1.236	1.95e-01	1.131
13154	0.088	13	1.00e-01	0.905	2.67e-01	1.051	1.78e-02	1.057	1.74e-02	1.393	8.91e-02	1.130
46082	0.047	11	5.44e-02	0.969	1.40e-01	1.026	9.35e-03	1.021	6.83e-03	1.491	4.55e-02	1.069
183962	0.024	9	2.74e-02	0.991	6.95e-02	1.011	4.65e-03	1.006	2.38e-03	1.521	2.23e-02	1.029
510602	0.014	8	1.65e-02	0.997	4.16e-02	1.004	2.79e-03	1.002	1.09e-03	1.526	1.33e-02	1.012

AFW$_\ell$–based discretization with $\ell = 0$												
DOF	h	it	e($\mathbf{D}$)	r($\mathbf{D}$)	e($\boldsymbol{\sigma}$)	r($\boldsymbol{\sigma}$)	e($\mathbf{u}$)	r($\mathbf{u}$)	e($\boldsymbol{\gamma}$)	r($\boldsymbol{\gamma}$)	e(p)	r(p)
609	0.354	15	5.62e-02	–	5.63e-01	–	6.94e-02	–	6.76e-02	–	3.27e-01	–
2369	0.177	14	2.65e-02	1.086	2.80e-01	1.005	3.48e-02	0.995	3.34e-02	1.018	1.63e-01	1.000
9345	0.088	12	1.30e-02	1.027	1.40e-01	1.002	1.74e-02	0.999	1.66e-02	1.006	8.17e-02	1.000
32641	0.047	10	6.89e-03	1.008	7.46e-02	1.001	9.29e-03	1.000	8.85e-03	1.002	4.36e-02	1.000
130081	0.024	7	3.44e-03	1.002	3.73e-02	1.001	4.65e-03	1.000	4.42e-03	1.001	2.18e-02	1.000
360801	0.014	6	2.06e-03	1.001	2.24e-02	1.001	2.79e-03	1.000	2.65e-03	1.000	1.31e-02	1.000

Table 7.1: [Example 1, $\ell = 0$] Number of degrees of freedom, meshsizes, Newton iteration count, errors, and rates of convergence for the mixed approximations.

PEERS$_\ell$–based discretization with $\ell = 1$												
DOF	h	it	e($\mathbf{D}$)	r($\mathbf{D}$)	e($\boldsymbol{\sigma}$)	r($\boldsymbol{\sigma}$)	e($\mathbf{u}$)	r($\mathbf{u}$)	e($\boldsymbol{\gamma}$)	r($\boldsymbol{\gamma}$)	e(p)	r(p)
1778	0.354	12	1.80e-02	–	4.59e-02	–	4.59e-03	–	7.45e-03	–	1.84e-02	–
7010	0.177	10	5.36e-03	1.750	1.17e-02	1.970	1.15e-03	1.999	3.12e-03	1.257	4.51e-03	2.031
27842	0.088	8	1.48e-03	1.858	2.98e-03	1.977	2.87e-04	2.001	9.81e-04	1.668	1.12e-03	2.006
97562	0.047	6	4.42e-04	1.922	8.56e-04	1.983	8.15e-05	2.000	3.09e-04	1.840	3.19e-04	1.998
389522	0.024	4	1.14e-04	1.958	2.16e-04	1.990	2.04e-05	2.000	8.16e-05	1.919	8.00e-05	1.997
1081202	0.014	4	4.14e-05	1.977	7.78e-05	1.993	7.34e-06	2.000	3.00e-05	1.957	2.88e-05	1.998

AFW$_\ell$–based discretization with $\ell = 1$												
DOF	h	it	e($\mathbf{D}$)	r($\mathbf{D}$)	e($\boldsymbol{\sigma}$)	r($\boldsymbol{\sigma}$)	e($\mathbf{u}$)	r($\mathbf{u}$)	e($\boldsymbol{\gamma}$)	r($\boldsymbol{\gamma}$)	e(p)	r(p)
1393	0.354	10	2.21e-03	–	2.49e-02	–	4.57e-03	–	2.84e-03	–	1.73e-02	–
5473	0.177	7	5.35e-04	2.046	6.12e-03	2.027	1.15e-03	1.997	7.29e-04	1.963	4.33e-03	1.996
21697	0.088	5	1.32e-04	2.020	1.52e-03	2.013	2.87e-04	1.999	1.84e-04	1.983	1.08e-03	1.999
75961	0.047	4	3.73e-05	2.009	4.29e-04	2.008	8.15e-05	2.000	5.27e-05	1.992	3.08e-04	2.000
303121	0.024	3	9.29e-06	2.007	1.07e-04	2.008	2.04e-05	2.000	1.32e-05	1.997	7.70e-05	2.000
841201	0.014	3	3.34e-06	2.002	3.84e-05	2.002	7.34e-06	2.000	4.76e-06	1.998	2.77e-05	2.000

Table 7.2: [Example 1, $\ell = 1$] Number of degrees of freedom, meshsizes, Newton iteration count, errors, and rates of convergence for the mixed approximations.

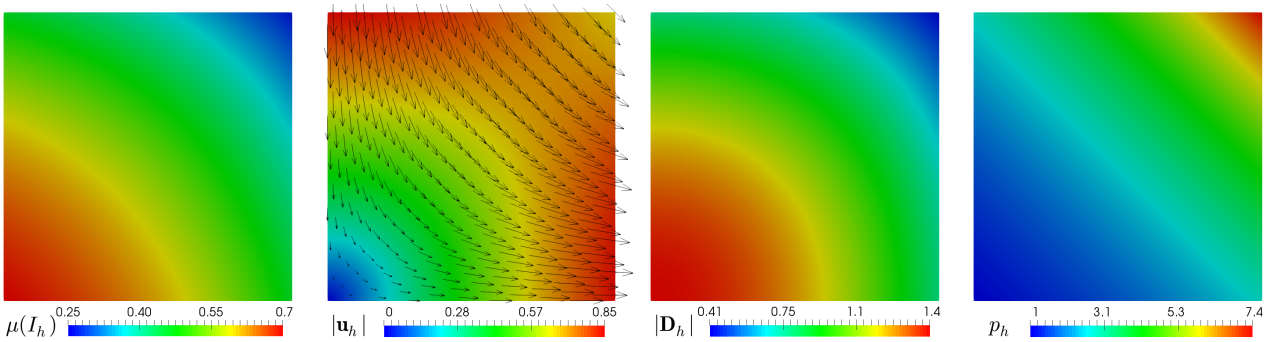

Figure 7.1: [Example 1] Computed internal friction coefficient, magnitude of the velocity and symmetric part of the velocity gradient, and pressure field.

Example 2: Convergence against smooth exact solutions in a 3D domain

In the second example we consider the cube domain $\Omega = (0,1)^3$, and the regularization factor $\varepsilon = 1E-06$. The manufactured solution is given by

$$\mathbf{u}(x_1,x_2,x_3) = \begin{pmatrix} \sin(x_1)\cos(x_2)\cos(x_3) \\ -2\cos(x_1)\sin(x_2)\cos(x_3) \\ \cos(x_1)\cos(x_2)\sin(x_3) \end{pmatrix} \quad \text{and} \quad p(x_1,x_2,x_3) = 10\,\exp(x_1+x_2+x_3)\,,$$

where $p \in \mathrm{L}^2_\kappa(\Omega)$, with $\kappa = 10\,(\exp(1)-1)^3$. Similarly to the first example, the data $\mathbf{f}$ and $\mathbf{u}_D$ is computed from (2.19) using the above solution. The convergence history for a set of quasi-uniform mesh refinements using $\ell = 0$ is shown in Table 7.3. Again, the mixed finite element method converges optimally with order $\mathcal{O}(h)$, as it was proved by Theorem 6.2. We observe a considerable increasing of degrees of freedom in the PEERS$_0$-based scheme compared to the AFW$_0$ one. This is justified mainly by the fact that the symmetric part of the velocity gradient is approximated with $\mathbb{P}_3(\Omega)$ and

$\mathbb{P}_1(\Omega)$, respectively. In addition, the discrete internal friction coefficient and some components of the numerical solution are displayed in Figure 7.2, which were built using the mixed AFW_0 approximation with meshsize $h = 0.108$ and $24,576$ tetrahedral elements (actually representing $1,390,081$ DOF).

PEERS$_\ell$-based discretization with $\ell = 0$												
DOF	h	it	e($\mathbf{D}$)	r($\mathbf{D}$)	e($\boldsymbol{\sigma}$)	r($\boldsymbol{\sigma}$)	e($\mathbf{u}$)	r($\mathbf{u}$)	e(γ)	r(γ)	e(p)	r(p)
8698	0.866	20	9.95e-01	–	5.05e+01	–	2.41e-01	–	6.04e-01	–	1.66e+01	–
69016	0.433	20	5.85e-01	0.766	2.73e+01	0.885	1.10e-01	1.135	2.28e-01	1.406	9.01e+00	0.884
550156	0.217	19	3.24e-01	0.852	1.36e+01	1.008	4.96e-02	1.143	7.95e-02	1.520	4.32e+00	1.061
1854688	0.144	18	2.23e-01	0.926	8.89e+00	1.046	3.19e-02	1.091	4.17e-02	1.590	2.74e+00	1.122
4393876	0.108	18	1.69e-01	0.957	6.59e+00	1.045	2.35e-02	1.056	2.62e-02	1.625	1.99e+00	1.113

AFW$_\ell$–based discretization with $\ell = 0$												
DOF	h	it	e($\mathbf{D}$)	r($\mathbf{D}$)	e($\boldsymbol{\sigma}$)	r($\boldsymbol{\sigma}$)	e($\mathbf{u}$)	r($\mathbf{u}$)	e(γ)	r(γ)	e(p)	r(p)
2905	0.866	12	2.09e-01	–	2.59e+01	–	1.78e-01	–	2.01e-01	–	1.43e+01	–
22369	0.433	11	8.24e-02	1.344	1.21e+01	1.104	9.12e-02	0.969	9.34e-02	1.103	7.15e+00	1.005
175489	0.217	9	3.56e-02	1.212	5.82e+00	1.050	4.59e-02	0.992	4.55e-02	1.037	3.57e+00	1.002
588385	0.144	8	2.28e-02	1.097	3.85e+00	1.023	3.06e-02	0.997	3.02e-02	1.014	2.38e+00	1.001
1390081	0.108	7	1.68e-02	1.054	2.87e+00	1.013	2.30e-02	0.999	2.26e-02	1.007	1.78e+00	1.000

Table 7.3: [Example 2, $\ell = 0$] Number of degrees of freedom, meshsizes, Newton iteration count, errors, and rates of convergence for the mixed approximations.

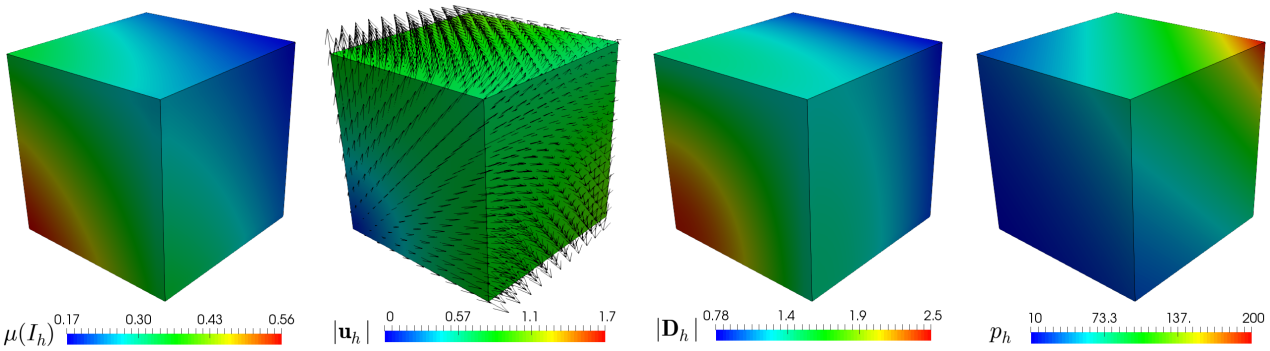

Figure 7.2: [Example 2] Computed internal friction coefficient, magnitude of the velocity and symmetric part of the velocity gradient, and pressure field.

Example 3: Fluid flow through a cavity 2D with a circular obstacle

In the last example, motivated by [30, Section 2.1], we study the behavior of the regularized $\mu(I)$-rheology model of granular materials for fluid flow through a cavity 2D with a circular obstacle without manufactured solution. More precisely, we consider the domain $\Omega = (0,1)^2 \setminus \Omega_c$, where

$$\Omega_c = \left\{ (x_1, x_2) : \quad (x_1 - 0.5)^2 + (x_2 - 0.5)^2 \ < \ 0.1^2 \ \right\},$$

with boundary Γ, whose part around the circle is given by $\Gamma_c = \partial\Omega_c$. The model parameters are chosen as $\mu_s = 0.36, \mu_d = 0.91, I_0 = 0.73, d = 0.05, \rho = 2500$, and the regularization factor is $\varepsilon = 1E-08$. Notice that the relation between the diameter of the particles d and the width of the cavity is $1:20$,

whereas the radius of the circular obstacle is double that of d. The mean value of p is fixed as $\kappa = 100$, no presence of gravity is assumed, that is, $\mathbf{f} = \mathbf{0}$, and the boundaries conditions are

$$\mathbf{u} = (2\,x_2 - 1, 0)^{\mathrm{t}} \quad \text{on} \quad \Gamma \setminus \Gamma_c \quad \text{and} \quad \mathbf{u} = \mathbf{0} \quad \text{on} \quad \Gamma_c\,.$$

In particular, we impose that flows cannot in nor out through Γ_c, whereas at the top and bottom of the domain flows are faster in opposite direction. In Figure 7.3, we display the computed internal friction coefficient, magnitude of the velocity and symmetric part of the velocity gradient, and pressure field, which were built using the mixed AFW$_0$-based scheme on a mesh with meshsize $h = 0.020$ and $12,433$ triangle elements (actually representing $224,441$ DOF). We observe higher velocities at the top and bottom of the boundary going to the right and left of the domain, respectively, as we expected. In addition, most of the variations in both the magnitude of the symmetric part of the velocity gradient tensor and pressure field occur around the circular obstacle. This observation aligns with the results obtained for the discrete internal friction coefficient. Notice also that at the middle of the domain the magnitude of the symmetric part of the velocity gradient is zero or close to it describing a region where the original viscosity η (2.9) is singular and hence the granular flows are static. The latter is in agreement with the velocity of the fluid and it is overcome by the mixed approximation considering the regularized viscosity (2.11) as it was described in Section 2.

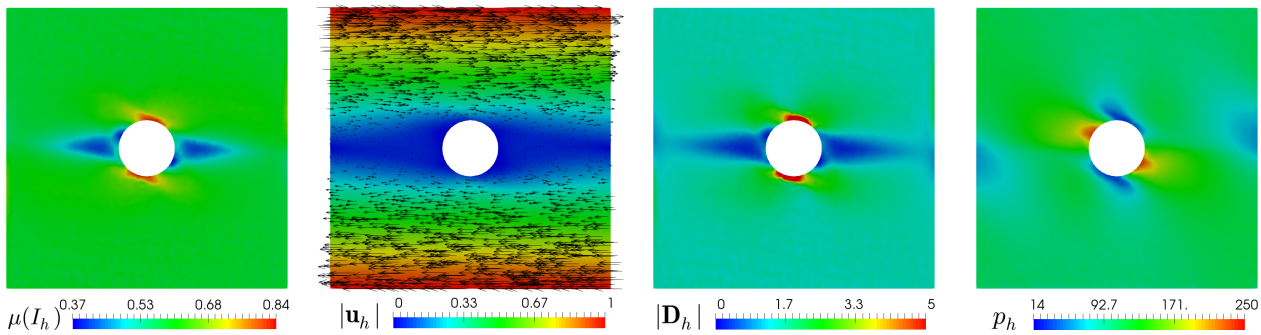

Figure 7.3: [Example 3] Computed internal friction coefficient, magnitude of the velocity and symmetric part of the velocity gradient, and pressure field.

A The hypotheses on the viscosity

In this appendix we refer to the regularized viscosity η and the corresponding fulfillment of the hypotheses (**H.1**), (**H.2**), and (**H.3**). We begin by recalling from (2.11) that

$$\eta(\varrho,\omega) := \frac{a_1\,\varrho}{\omega+\varepsilon} + \frac{a_2\,\varrho}{a_3\,\sqrt{\varrho}+a_4\,\omega+\varepsilon} \qquad \forall\,(\varrho,\omega)\in \mathrm{R}^+\times\mathrm{R}^+\,, \tag{A.1}$$

so that

$$\frac{\partial}{\partial\omega}\eta(\varrho,\omega) = -\frac{a_1\,\varrho}{(\omega+\varepsilon)^2} - \frac{a_2\,a_4\,\varrho}{(a_3\,\sqrt{\varrho}+a_4\,\omega+\varepsilon)^2} \qquad \forall\,(\varrho,\omega)\in \mathrm{R}^+\times\mathrm{R}^+\,, \tag{A.2}$$

and then

$$\eta(\varrho,\omega) + \omega\frac{\partial}{\partial\omega}\eta(\varrho,\omega) = \frac{a_1\,\varrho\,\varepsilon}{(\omega+\varepsilon)^2} + \frac{a_2\,(a_3\,\sqrt{\varrho}+\varepsilon)\,\varrho}{(a_3\,\sqrt{\varrho}+a_4\,\omega+\varepsilon)^2} \qquad \forall\,(\varrho,\omega)\in \mathrm{R}^+\times\mathrm{R}^+\,. \tag{A.3}$$

Thus, in order to satisfy (**H.1**) and (**H.2**), we restrict the evaluation of η, as defined by (A.1), to a given rectangle $[\varrho_1, \varrho_2] \times [\omega_1, \omega_2] \subseteq \mathrm{R}^+ \times \mathrm{R}^+$, so that η is extended by continuity outside this region, as illustrated in Figure A.1 below.

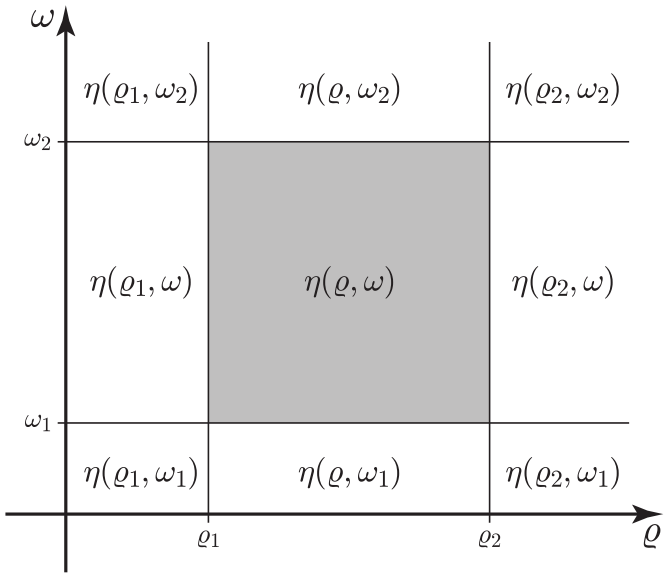

Figure A.1: Graphic representation of the modified version of the viscosity function η.

In this way, it is possible to accomplish the aforementioned hypotheses with positive constants η_1 and η_2, depending on ϱ_1, ϱ_2, ω_1, ω_2, ε, and the coefficients a_i, $i \in \{1, ..., 4\}$, defined in (2.10). Note also that, under this modification, one could even get rid of the parameter ε.

On the other hand, regarding (**H.3**), we show next that it is satisfied with a positive constant L_η depending only on the coefficients a_1, a_2, and a_4 (cf. (2.10)). Indeed, given ϱ, χ, and ω in R^+, we first deduce from (A.1) and some algebraic manipulations, that

$$\begin{aligned} &\Big\{\eta(\varrho,\omega) - \eta(\chi,\omega)\Big\}\,\omega \\ &\quad = \left\{\frac{a_1\,\omega}{\omega+\varepsilon} + \frac{a_2\,a_3\,\sqrt{\varrho}\,\sqrt{\chi}\,\omega}{(\sqrt{\varrho}+\sqrt{\chi})\,\mathbf{a}(\varrho,\omega,\varepsilon)\,\mathbf{a}(\chi,\omega,\varepsilon)} + \frac{a_2\,\omega\,(a_4\,\omega+\varepsilon)}{\mathbf{a}(\varrho,\omega,\varepsilon)\,\mathbf{a}(\chi,\omega,\varepsilon)}\right\}(\varrho-\chi)\,, \end{aligned} \tag{A.4}$$

where

$$\mathbf{a}(\varrho,\omega,\varepsilon) \,:=\, a_3\,\sqrt{\varrho} + a_4\,\omega + \varepsilon\,,$$

and analogously for $\mathbf{a}(\chi,\omega,\varepsilon)$. In order to bound the right-hand side of (A.4) we first observe that

$$\frac{a_1\,\omega}{\omega+\varepsilon} \,\leqslant\, a_1\,. \tag{A.5}$$

Then, it is straightforward to show that

$$\begin{aligned} &\frac{\sqrt{\varrho}}{\sqrt{\varrho}+\sqrt{\chi}} \,\leqslant\, 1\,, \qquad \frac{a_3\,\sqrt{\chi}}{\mathbf{a}(\chi,\omega,\varepsilon)} \,=\, \frac{a_3\,\sqrt{\chi}}{a_3\,\sqrt{\chi}+a_4\,\omega+\varepsilon} \,\leqslant\, 1\,, \quad \text{and} \\ &\qquad\qquad \frac{a_2\,\omega}{\mathbf{a}(\varrho,\omega,\varepsilon)} \,=\, \frac{a_2\,a_4\,\omega}{a_4\,(a_3\,\sqrt{\varrho}+a_4\,\omega+\varepsilon)} \,\leqslant\, \frac{a_2}{a_4}\,, \end{aligned} \tag{A.6}$$

which yield

$$\frac{a_2\, a_3\, \sqrt{\varrho}\, \sqrt{\chi}\, \omega}{(\sqrt{\varrho} + \sqrt{\chi})\, \mathbf{a}(\varrho, \omega, \varepsilon)\, \mathbf{a}(\chi, \omega, \varepsilon)} \leqslant \frac{a_2}{a_4}\,. \tag{A.7}$$

In turn, it is readily seen that

$$\frac{a_4\, \omega + \varepsilon}{\mathbf{a}(\chi, \omega, \varepsilon)} = \frac{a_4\, \omega + \varepsilon}{a_3\, \sqrt{\chi} + a_4\, \omega + \varepsilon} \leqslant 1\,,$$

which, along with the third inequality from (A.6), imply

$$\frac{a_2\, \omega\, (a_4\, \omega + \varepsilon)}{\mathbf{a}(\varrho, \omega, \varepsilon)\, \mathbf{a}(\chi, \omega, \varepsilon)} \leqslant \frac{a_2}{a_4}\,. \tag{A.8}$$

Finally, employing (A.5), (A.7), and (A.8) in (A.4), we arrive at

$$\big|\eta(\varrho, \omega) - \eta(\chi, \omega)\big|\, \omega \leqslant L_\eta\, |\varrho - \chi|\,, \tag{A.9}$$

where, using (2.10),

$$L_\eta := a_1 + \frac{2\, a_2}{a_4} = \big(2\, \mu_d - \mu_s\big)\, \sqrt{2}\,,$$

thus proving (**H.3**).

References

[1] M.S. Alnaes, J. Blechta, J. Hake, A. Johansson, B. Kehlet, A. Logg, C. Richardson, J. Ring, M.E. Rognes, and G.N. Wells, *The FEniCS project version 1.5*. Arch. Numer. Softw. 3 (2015) 9–23.

[2] B. Andreotti, Y. Forterre and O. Pouliquen, *Granular Media: Between Fluid and Solid*. Cambridge University Press, 2013.

[3] D.N. Arnold, F. Brezzi and J. Douglas, PEERS: *A new mixed finite element method for plane elasticity*. Jpn. J. Appl. Math. 1 (1984), 347–367.

[4] D.N. Arnold, R.S. Falk and R. Winther, *Mixed finite element methods for linear elasticity with weakly imposed symmetry¿* Math. Comp. 76 (2007), no. 260, 1699–1723.

[5] T. Barker, D.G. Schaeffer, P. Bohorquez and J.M.N.T. Gray, *Well-posed and ill-posed behaviour of the $\mu(I)$-rheology for granular flow*. J. Fluid Mech. 779 (2015), 794–818.

[6] G.A. Benavides, S. Caucao, G.N. Gatica and A.A. Hopper, *A Banach spaces–based analysis of a new mixed–primal finite element method for a coupled flow–transport problem*. Comput. Methods Appl. Mech. Engrg. 371 (2020), 113285.

[7] I. Bermúdez, C.I. Correa, G.N. Gatica and J.P. Silva, *A perturbed twofold saddle point-based mixed finite element method for the Navier-Stokes equations with variable viscosity*. Preprint 2023-19, Centro de Investigación en Ingeniería Matemática, Universidad de Concepción, Chile, (2023).

[8] D. Boffi, F. Brezzi and M. Fortin, Mixed Finite Element Methods and Applications. Springer Series in Computational Mathematics, 44. Springer, Heidelberg, 2013.

[9] F. Brezzi and M. Fortin, Mixed and Hybrid Finite Element Methods. Springer-Verlag, 1991.

[10] J. Camaño, C. García and R. Oyarzúa, *Analysis of a momentum conservative mixed-FEM for the stationary Navier-Stokes problem.* Numer. Methods Partial Differential Equations 37 (2021), no. 5, 2895–2923.

[11] J. Camaño, C. Muñoz and R. Oyarzúa, *Numerical analysis of a dual-mixed problem in non-standard Banach spaces.* Electron. Trans. Numer. Anal. 48 (2018), 114–130.

[12] S. Caucao, G.N. Gatica and F. Sandoval, *A fully-mixed finite element method for the coupling of the Navier-Stokes and Darcy-Forchheimer equations.* Numer. Methods Partial Differential Equations 37 (2021), no. 3, 2550–2587.

[13] S. Caucao, R. Oyarzúa and S. Villa-Fuentes, *A new mixed-FEM for steady-state natural convection models allowing conservation of momentum and thermal energy.* Calcolo 57 (2020), no. 4, Paper No. 36.

[14] S. Caucao and I. Yotov, *A Banach space mixed formulation for the unsteady Brinkman-Forchheimer equations.* IMA J. Numer. Anal. 41 (2021), no. 4, 2708–2743.

[15] J. Chauchat and M. Médale, *A three-dimensional numerical model for dense granular flows based on the $\mu(I)$ rheology.* J. Comput. Phys. 256 (2014), 696–712.

[16] E. Colmenares, G.N. Gatica and S. Moraga, *A Banach spaces-based analysis of a new fully-mixed finite element method for the Boussinesq problem.* ESAIM Math. Model. Numer. Anal. 54 (2020), no. 5, 1525–1568.

[17] E. Colmenares, G.N. Gatica and J.C. Rojas, *A Banach spaces-based mixed-primal finite element method for the coupling of Brinkman flow and nonlinear transport.* Calcolo 59 (2022), no. 4, Paper No. 51.

[18] E. Colmenares and M. Neilan, *Dual-mixed finite element methods for the stationary Boussinesq problem.* Comp. Math. Appl. 72 (2016), no. 7, 1828–1850.

[19] P.A. Cundall and O.D.L. Strack, *A discrete numerical model for granular assemblies.* Geotechnique 29 (1979), 47–65.

[20] A. Ern and J.-L Guermond, Theory and Practice of Finite Elements. Applied Mathematical Sciences, 159. Springer-Verlag, New York, 2004.

[21] A. Franci and M. Cremonesi, *3D regularized $\mu(I)$-rheology for granular flows simulation.* J. Comp. Phys. 378 (2019), 257–277.

[22] G.N. Gatica, A Simple Introduction to the Mixed Finite Element Method. Theory and Applications. SpringerBriefs in Mathematics. Springer, Cham, 2014.

[23] G. N. Gatica, N. Heuer, and S. Meddahi, *On the numerical analysis of nonlinear twofold saddle point problems.* IMA J. Numer. Anal. 23 (2003), no. 2, 301–330.

[24] G.N. Gatica, N. Núñez and R. Ruiz-Baier, *New non-augmented mixed finite element methods for the Navier-Stokes-Brinkman equations using Banach spaces.* J. Numer. Math. 31 (2023), no.4, 343–373.

[25] G.N. Gatica, R. Oyarzúa, R. Ruiz-Baier and Y.D. Sobral, *Banach spaces-based analysis of a fully-mixed finite element method for the steady-state model of fluidized beds*. Comput. Math. Appl. 84 (2021), 244–276.

[26] G.N. Gatica and W.L. Wendland, *Coupling of mixed finite elements and boundary elements for linear and nonlinear elliptic problems*. Appl. Anal. 63 (1996), no. 1-2, 39–75.

[27] GDR-MiDi, *On dense granular flows*. European Journal of Physics E 14 (2004), 341–365.

[28] E.J. Hinch, *Think before you compute: a prelude to computational fluid dynamics*. Cambridge University Press, 2021.

[29] L. Jing, C.Y. Kwok, Y.F. Leung and Y.D. Sobral, *Characterization of base roughness for granular chute flows*. Physical Review E 94 (2016), 052901.

[30] L. Jing, J.M. Ottino, P.B. Umbanhowar and R.M. Lueptow, *Drag force in granular shear flows: regimes, scaling laws and implications for segregation*. J. Fluid Mech. 948 (2022), A24.

[31] P. Jop, Y. Forterre and O. Pouliquen, *A constitutive law for dense granular flows*. Nature 441 (2008), no. 8, 727–730.

[32] R.R. Kerswell, *Dam break with Coulomb friction: A model for granular slumping ?*. Physics of Fluids 17 (5) (2005) 057101.

[33] P.Y. Lagree, L. Staron and S. Popinet, *The granular column collapse as a continuum: validity of a two-dimensional Navier–Stokes model with a $\mu(I)$-rheology*. J. Fluid Mech. 686 (2011), 378–408.

[34] M. Lonsing and R. Verfürth, *On the stability of* BDMS *and* PEERS *elements*. Numer. Math. 99 (2004), no. 1, 131–140.

[35] S.B. Savage and K. Hutter, *The motion of a finite mass of granular material down a rough incline*. J. Fluid Mech. 199 (1989), 177–215.

[36] L. Staron, P.-Y. Lagrée and S. Popinet, *Continuum simulation of the discharge of the granular silo*. European Journal of Physics E 37 (2014), 5.

Centro de Investigación en Ingeniería Matemática (CI^{2}MA)

PRE-PUBLICACIONES 2023 - 2024

2023-21 Boumediene Chentouf, Aissa Guesmia, Mauricio Sepúlveda, Rodrigo Véjar: *Boundary stabilization of the Korteweg-de Vries-Burgers equation with an infinite memory-type control and applications: a qualitative and numerical analysis*

2023-22 Franz Chouly: *A short journey into the realm of numerical methods for contact in elastodynamics*

2023-23 Stéphane P. A. Bordas, Marek Bucki, Huu Phuoc Bui, Franz Chouly, Michel Duprez, Arnaud Lejeune, Pierre-Yves Rohan: *Automatic mesh refinement for soft tissue*

2023-24 Mauricio Sepúlveda, Nicolás Torres, Luis M. Villada: *Well-posedness and numerical analysis of an elapsed time model with strongly coupled neural networks*

2023-25 Franz Chouly, Patrick Hild, Yves Renard: *Lagrangian and Nitsche methods for frictional contact*

2023-26 Sergio Caucao, Gabriel N. Gatica, Juan P. Ortega: *A three-field mixed finite element method for the convective Brinkman–Forchheimer problem with varying porosity*

2023-27 Raimund Bürger, Yessennia Martínez, Luis M. Villada: *Front tracking and parameter identification for a conservation law with a space-dependent coefficient modeling granular segregation*

2023-28 Marie Haghebaert, Beatrice Laroche, Mauricio Sepúlveda: *Study of the numerical method for an inverse problem of a simplified intestinal crypt*

2023-29 Rodolfo Araya, Fabrice Jaillet, Diego Paredes, Frederic Valentin: *Generalizing the Multiscale Hybrid-Mixed Method for Reactive-Advective-Diffusive Equations*

2023-30 Jessika Camaño, Ricardo Oyarzúa, Miguel Serón, Manuel Solano: *A mass conservative finite element method for a nonisothermal Navier-Stokes/Darcy coupled system*

2023-31 Franz Chouly, Hao Huang, Nicolás Pignet: *HHT-α and TR-BDF2 schemes for Nitsche-based discrete dynamic contact*

2024-01 Sergio Caucao, Gabriel N. Gatica, Saulo Medrado, Yuri D. Sobral: *Nonlinear twofold saddle point-based mixed finite element methods for a regularized $\mu(I)$-rheology model of granular materials*

Para obtener copias de las Pre-Publicaciones, escribir o llamar a: Director, Centro de Investigación en Ingeniería Matemática, Universidad de Concepción, Casilla 160-C, Concepción, Chile, Tel.: 41-2661324, o bien, visitar la página web del centro: `http://www.ci2ma.udec.cl`







Centro de Investigación en
Ingeniería Matemática (CI²MA)
Universidad de Concepción

Casilla 160-C, Concepción, Chile
Tel.: 56-41-2661324/2661554/2661316
http://www.ci2ma.udec.cl